JOC Article

Multi-Mannosides Based on a Carbohydrate Scaffold: Synthesis, Force Field Development, Molecular Dynamics Studies, and Binding Affinities for Lectin Con A

Sébastien G. Gouin,*,† Enguerran Vanquelef,‡ José Manuel García Fernández,§ Carmen Ortiz Mellet,*,|| François-Yves Dupradeau,*,‡ and José Kovensky*,†

Laboratoire des Glucides UMR CNRS 6219, Faculté des Sciences, Université de Picardie Jules Verne, 33 Rue Saint-Leu, 80039 Amiens Cedex 1, France, DMAG, EA 3901, Faculté de Pharmacie et de Médecine, Université de Picardie Jules Verne, 1-3 Rue des Louvels, 80037 Amiens Cedex 1, France, Instituto de Investigaciones Químicas, CSIC, Américo Vespucio 49, Isla de la Cartuja, 41092 Sevilla, Spain, and Departamento de Química Orgánica, Facultad de Química, Universidad de Sevilla, Apartado 553, 41071 Sevilla, Spain

jose.kovensky@u-picardie.fr

Received June 12, 2007

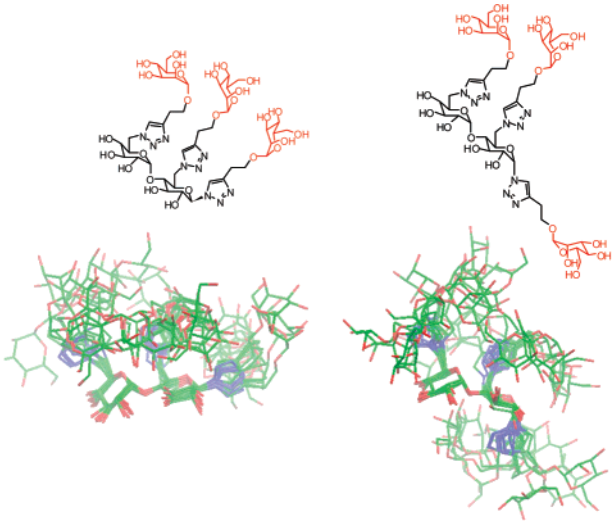

A short and efficient strategy for the synthesis of multi-valent mannosides based on a selectively functionalized carbohydrate scaffold was reported involving (i) direct regioselective azidation of unprotected commercial saccharides, (ii) acetylation, (iii) grafting of the mannosyl ligands by click chemistry, and (iv) deacetylation. New glycoclusters with a valency ranging from 1 to 4 and different spatial arrangements of the epitopes were obtained. Binding affinities of the new glycoclusters toward concanavalin A (Con A) lectin were investigated by an enzyme-linked lectin essay (ELLA). The synthetic multi-valent compounds exhibited a remarkable cluster effect with a relative potency per mannoside residue ranging from 8.1 to 9.1 depending on the structures. ELLA experiments were in agreement with the establishment of favorable interactions between triazole ring and Con A, increasing the binding affinity. A new force field topology database was developed in agreement with the GLYCAM 2004 force field. Molecular dynamics performed on representative glyco-conjugates revealed interesting structural features such as rigidity of the scaffold for a well-defined presentation of the ligands and highly flexible mannose counterparts. The new glycoconjugates reported may be promising tools as probes or effectors of biological processes involving lectins.

Introduction

Carbohydrate−lectin interactions play a pivotal role in many biological events including inflammation,[1] immune response, apoptosis, tumor metastasis, or viral and bacterial infections.[2,3] The generally low affinity of monovalent ligands for their putative lectins can be overcome by using polyfunctional scaffolds displaying structurally well-defined saccharide units.

* Corresponding authors. (S.G.G. and J.K.) Fax: (+33) 3 22827568. (C.O.M.) Fax: (+34) 954-624-960. (F.-Y.D.) Fax: (+33) 3 22827469.
† Faculté des Sciences, Université de Picardie Jules Verne.
‡ Faculté de Pharmacie et de Médecine, Université de Picardie Jules Verne.
§ Instituto de Investigaciones Químicas.
|| Universidad de Sevilla.

(1) (a) Hanessian, S.; Mascitti, V.; Rogel, O. *J. Org. Chem.* **2002**, *67*, 3346−3354. (b) Murphy, P. V.; Hubbard, R. E.; Manallack, D. T.; Wills, R. E.; Montana, J. G.; Taylor, R. J. K. *Bioorg. Med. Chem.* **1998**, *6*, 2421−2439.

10.1021/jo071248a CCC: $37.00
Published on Web 11/03/2007

The affinity enhancements reached by using this strategy can be very impressive.[4,5] A remarkable example is the decavalent ligand designed by Bundle and co-workers (STARFISH), which inhibited Shiga-like toxins in ELISA assays with a 10^6-fold enhancement over the monomeric species.[6]

Depending both on the nature of the receptor and on the valence and geometry of the ligand, this gain in stability, the so-called multi-valent or cluster effect,[7] can be explained by the interplay of different mechanisms, including a chelation binding mode, clustering of receptors, or statistical rebinding.[8] Hundreds of synthetic multi-valent glycomimetics with diverse spatial arrangements, number of epitopes, and degrees of freedom have been synthesized. Such glycoconjugates have been classified as glycodendrimers, glycoclusters, glycopolymers, and glycoproteins depending on the nature of their scaffold. Different reactions have been used for grafting the sugar epitopes (e.g., glycosilation,[9] peptidic coupling, thiourea and oxime bond formation,[10,11] Sonogashira coupling,[12] photochemically promoted radical addition of thiols to double bonds,[13] and the Huisgen 1,3-dipolar cycloaddition).[14] The last reaction, also referred to as "click chemistry", owes its usefulness in part to its high compatibility with a broad range of functional groups (e.g., alcohols, carboxylic acids, and amines) in different solvent systems, including water.[15] Furthermore, the generated triazole ring is stable to hydrolytic cleavage and virtually inert toward oxidation or reduction.[16]

Carbohydrates have not been investigated much as scaffolds as compared to dendrimers or polymers.[8,17] Most of the examples on record correspond to glycosylamide scaffolds and cyclomaltooligosaccharide (cyclodextrin)-centered glycoclusters.[18,19] The use of nonreducing mono- or disaccharide templates where all hydroxyl groups have been elaborated to graft sugar epitopes has also been explored.[20] For in vivo applications, however, multi-valent ligands based on carbohydrate scaffolds keeping some free hydroxyl groups may be more appropriate. Improved hydrophilicity and pharmacokinetics may be expected, for instance, as compared to peptidic, aromatic, or polymeric scaffolds.[13a,21] Following our ongoing interest in the use of click chemistry for the synthesis of neoglycoconjugates,[22] we present herein the preparation of new multi-mannosides from regioselectively modified mono-, di-, and trisaccharide templates. The binding affinities of these glycoconjugates toward the mannose-specific lectin concanavalin A (Con A) were evaluated by enzyme-linked lectin assay (ELLA).[23] To rationalize the observed affinities, molecular dynamics (MD) calculations were performed on four representative structures.

Results and Discussion

Synthesis of Multi-Mannosides on Carbohydrate Scaffold. Commercially available maltose and maltotriose were considered as polyfunctional cores to generate multi-valency. Regioselective polyazidation of the fully unprotected sugars was performed in one pot by using triphenylphosphine/carbon tetrabromide/sodium azide in dry DMF as the azidation system.[24] The number and the position of the azido groups in the final compound can be modulated by varying the relative proportions of reagents

(2) (a) Rabinovich, G. A. *Cell Death Differ.* **1999**, *6*, 711−721. (b) Ochieng, J.; Furtack, V. *Glycoconjugate J.* **2004**, *19*, 527−535.

(3) For reviews on lectins: (a) Lis, H.; Sharon, N. *Chem. Rev.* **1998**, *98*, 637−674. (b) Gabius, H.-J. *Adv. Drug Delivery Rev.* **2004**, *56*, 421−424. (c) Gabius, H.-J.; André, S.; Kaltner, H.; Siebert, H.-C. *Biochim. Biophys. Acta* **2002**, *1572*, 165−177. (d) Ambrosi, M.; Cameron, N. R.; Davis, B. G. *Org. Biomol. Chem.* **2005**, *3*, 1593−1608.

(4) Vrasidas, I.; André, S.; Valentini, P.; Böck, C.; Lensch, M.; Kaltner, H.; Liskamp, R. M. J.; Gabius, H.-J.; Pieters, R. J. *Org. Biomol. Chem.* **2003**, *1*, 803−810.

(5) (a) Zhang, Z.; Merritt, E. A.; Ahn, M.; Roach, C.; Hou, Z.; Verlinde, C. L. M. J.; Hol, W. G. J.; Fan, E. *J. Am. Chem. Soc.* **2002**, *124*, 12991−12998. (b) Fan, E.; Zhang, Z.; Minke, W. E.; Hou, Z.; Verlinde, C. L. M. J.; Hol, W. G. J. *J. Am. Chem. Soc.* **2000**, *122*, 2663−2664.

(6) Kitov, P. I.; Sadowska, J. M.; Mulvey, G.; Arnstrong, G. D.; Ling, H.; Pannu, N. S.; Read, R. J.; Bundle, D. R. *Nature (London, U.K.)* **2000**, *403*, 669−672.

(7) (a) Lundquist, J. J.; Toone, E. J. *Chem. Rev.* **2002**, *102*, 555−578. (b) Lee, R. T.; Lee, Y. C. *Glycoconjugate J.* **2000**, *17*, 543−551. (c) Mammen, M.; Choi, S.-K.; Whitesides, G. M. *Angew. Chem., Int. Ed.* **1998**, *37*, 2754−2794. (d) Lee, Y. C.; Lee, R. T. *Acc. Chem. Res.* **1995**, *28*, 321−327.

(8) Kiessling, L. L.; Gestwicki, J. E.; Strong, L. E. *Angew. Chem., Int. Ed.* **2006**, *45*, 2348−2368.

(9) Dubber, M.; Sperling, O.; Lindhorst, T. K. *Org. Biomol. Chem.* **2006**, *4*, 3901−3912.

(10) (a) Wolfenden, M. L.; Cloninger, M. J. *J. Am. Chem. Soc.* **2005**, *127*, 12168−12169. (b) Patel, A.; Lindhorst, T. K. *Carbohydr. Res.* **2006**, *341*, 1657−1668.

(11) Singh, Y.; Renaudet, O.; Defrancq, E.; Dumy, P. *Org. Lett.* **2005**, *7*, 1359−1362.

(12) André, S.; Liu, B.; Gabius, H.-J.; Roy, R. *Org. Biomol. Chem.* **2003**, *1*, 3909−3916.

(13) (a) Köhn, M.; Benito, J. M.; Mellet, C. O.; Lindhorst, T. K.; García Fernández, J. M. *ChemBioChem* **2004**, *5*, 771−777. (b) Fulton, D. A.; Stoddart, J. F. *J. Org. Chem.* **2001**, *66*, 8309−8319.

(14) (a) Wu, P.; Fokin, V. V. *Aldrichimica Acta* **2007**, *40*, 7−17. (b) Nepogodiev, S. A.; Dedola, S.; Marmuse, L.; de Oliveira, M. T.; Field, R. A. *Carbohydr. Res.* **2007**, *342*, 529−540. (c) Ballell, L.; van Scherpenzeel, M.; Buchalova, K.; Liskamp, R. M. J.; Pieters, R. J. *Org. Biomol. Chem.* **2006**, *4*, 4387−4394. (d) Pérez-Balderas, F.; Hernández-Mateo, F.; Santoyo-González, F. *Tetrahedron* **2005**, *61*, 9338−9348.

(15) Bock, V. D.; Hiemstra, H.; van Maarseveen, J. H. *Eur. J. Org. Chem.* **2006**, *1*, 51−68.

(16) Kolb, H. C.; Sharpless, K. B. *Drug Discovery Today* **2003**, *8*, 1128−1137.

(17) (a) Hashimoto, M.; Morimoto, M.; Saimoto, H.; Shigemasa, Y.; Sato, T. *Bioconjugate Chem.* **2006**, *17*, 309−316. (b) Nelson, A.; Stoddart, J. F. *Carbohydr. Res.* **2004**, *339*, 2069−2075. (c) Kalovidouris, S. A.; Blixt, O.; Nelson, A.; Vidal, S.; Turnbull, W. B.; Paulson, J. C.; Stoddart, J. F. *J. Org. Chem.* **2003**, *68*, 8485−8493. (d) Turnbull, W. B.; Kalovidouris, S. A.; Stoddart, J. F. *Chem.—Eur. J.* **2002**, *8*, 2988−3000. (e) Turnbull, W. B.; Pease, A. R.; Stoddart, J. F. *ChemBioChem.* **2000**, *1*, 70−74. (f) Colonna, B.; Harding, V. D.; Nepogodiev, S. A.; Raymo, F. M.; Spencer, N.; Stoddart, J. F. *Chem.—Eur. J.* **1998**, *4*, 1244−1254.

(18) (a) Murphy, P. V.; Bradley, H.; Tosin, M.; Pitt, N.; Fitzpatrick, G. M.; Glass, W. K. *J. Org. Chem.* **2003**, *68*, 5692−5704. (b) Velasco-Torrijos, T.; Murphy, P. V. *Org. Lett.* **2004**, *6*, 3961−3964. (c)Tosin, M.; Gouin, S. G.; Murphy, P. V. *Org. Lett.* **2005**, *7*, 211−214. (d)Tosin, M.; Murphy, P. V. *J. Org. Chem.* **2005**, *70*, 4107−4117.

(19) For reviews, see: (a) Vargas-Berenguel, A.; Ortega-Caballero, F.; Casas-Solvas, J. M. *Mini-Rev. Org. Chem.* **2007**, *4*, 1−14. (b) Ortiz Mellet, C.; Defaye, J.; García Fernández, J. M. *J. Incl. Phenom. Macrocycl. Chem.* **2006**, *56*, 149−159. (c) Ortiz Mellet, C.; Defaye, J.; García Fernández, J. M. *Chem.—Eur. J.* **2002**, *8*, 1982−1990.

(20) (a) Sperling, O.; Fuchs, A.; Lindhorst, T. K. *Org. Biomol. Chem.* **2006**, *4*, 3913−3922. (b) Gao, Y.; Eguchi, A.; Kakehi, K.; Lee, Y. C. *Bioorg. Med. Chem.* **2005**, *13*, 6151−6157.

(21) (a) Haubner, R.; Wester, H.-J.; Burkhart, F.; Senekowitsch-Schmidtke, R.; Weber, W.; Goodman, S. L.; Kessler, H.; Schwaiger, M. *J. Nucl. Med.* **2001**, *42*, 326−336. (b) Beer, A. J.; Haubner, R.; Goebel, M.; Luderschmidt, S.; Spikler, M. E.; Wester, H.-J.; Weber, W. A.; Schwaiger, M. *J. Nucl. Med.* **2005**, *46*, 1333−1341.

(22) Gouin, S. G.; Bultel, L.; Falentin, C.; Kovensky, J. *Eur. J. Org. Chem.* **2007**, *7*, 1160−1167.

(23) For selected examples of applications of the ELLA protocol, see: (a) Smiljanic, N.; Moreau, V.; Yockot, D.; Benito, J. M.; García Fernández, J. M.; Djedaïni-Pilard, F. *Angew. Chem., Int. Ed.* **2006**, *45*, 5465−5468. (b) Benito, J. M.; Gómez-García, M.; Ortiz Mellet, C.; Baussanne, I.; Defaye, J.; García Fernández, J. M. *J. Am. Chem. Soc.* **2004**, *126*, 10355−10366. (c) Corbell, J. B.; Lundquist, J. J.; Toone, E. J. *Tetrahedron: Asymmetry* **2000**, *11*, 95−111. (d) Roy, R.; Pagé, D.; Figueroa Pérez, S.; Verez Bencomo, V. *Glycoconjugate J.* **1998**, *15*, 251−263.

(24) (a) Gouin, S. G.; Kovensky, J. *Tetrahedron Lett.* **2007**, *48*, 2875−2879. (b) Jiménez-Blanco, J. L.; García Fernández, J. M.; Gadelle, A.; Defaye, J. *Carbohydr. Res.* **1997**, *303*, 367−372.

SCHEME 1. Direct Azidation of Maltose

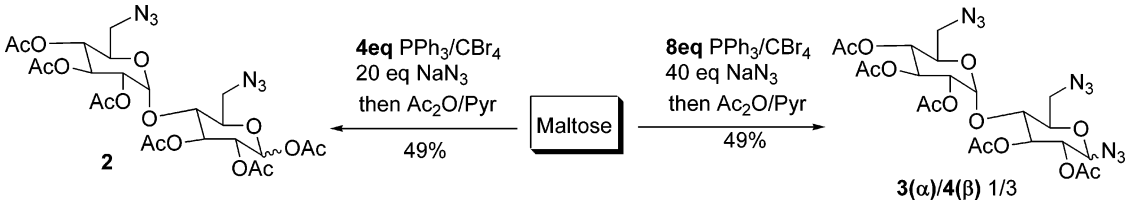

CHART 1. Structure of Azido Compounds 1−7

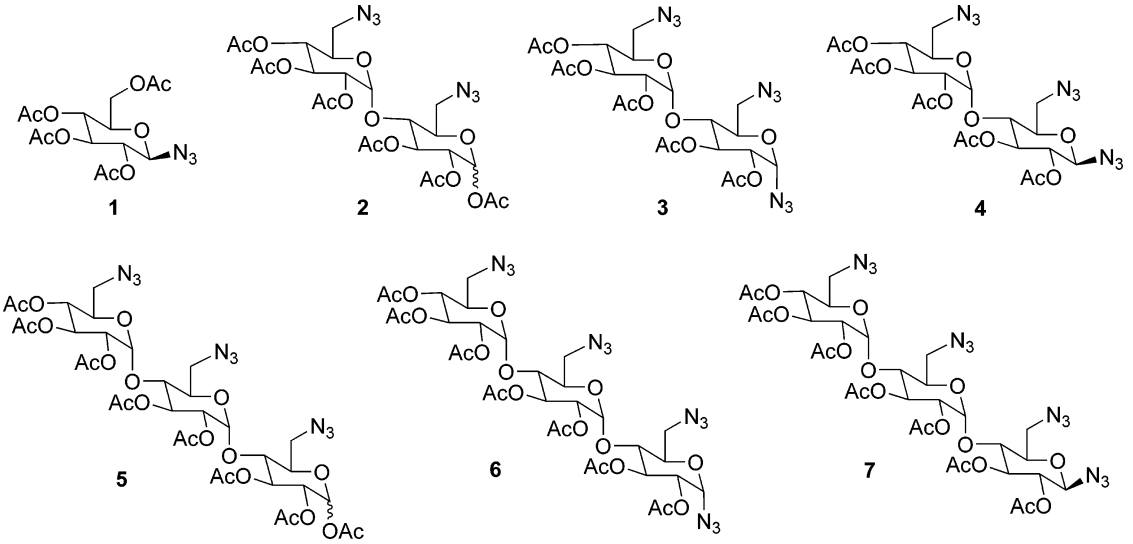

SCHEME 2. Synthesis of Cycloadduct 9 by Click Chemistry

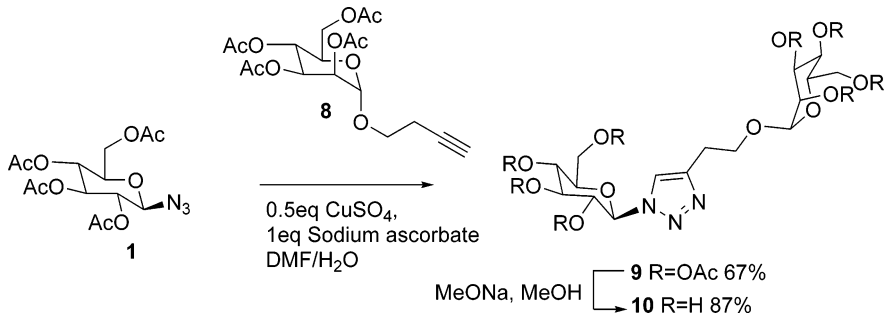

(Scheme 1). The crude reaction mixtures were per-O-acetylated with acetic anhydride-pyridine prior to chromatographic purification. Despite moderate yields, the direct azidation−acetylation methodology is of practical value as compared to alternative multi-step syntheses employed for accessing polyazidosugars.

The ensemble of azidosugars synthesized by this procedure is presented in Chart 1. Glucopyranosyl azide **1**[25] and azidosugars **2** and **5** were obtained from D-glucose, maltose, and maltotriose in 31, 49, and 41% yields, respectively, by using a 2:2:10 $PPh_3/CBr_4/NaN_3$ molar proportion per monosaccharide unit, followed by acetylation. When the proportion of the azidation reagent was increased to 4:4:20, the same protocol allowed isolation of the anomeric mixture **3**(α)/**4**(β) from maltose and **6**(α)/**7**(β) from maltotriose in 39 and 26% yields, repectively. In both cases, the per-O-acetylated anomers could be separated by flash chromatography.

To check the suitability of the prepared (poly)azidosugars for click chemistry glycocoating strategies, the alkynyl mannoside **8** was considered as a suitable partner. Compound **8** was synthesized from the corresponding peracetylated monosaccharide by treatment with but-3-yn-1-ol in the presence of boron trifluoride etherate.[26] The first cycloaddition trial was performed with **8** and acetylated glucopyranosyl azide **1** (Scheme 2). Cycloadduct **9** could be obtained using sodium ascorbate and copper sulfate as a catalyst in a 4:1 mixture of DMF and water.[22] Using DMF instead of the commonly used alcohols, such as *t*-butanol, was found to be generally advantageous in terms of better solubilization of the substrates and faster reaction times. Water has a positive effect on the reaction as previously reported.[27] Indeed, no cycloaddition product was formed if the reaction was conducted in dry DMF using the same proportions of reagents and reactants. Final deacetylation was carried out with sodium methanolate in methanol using standard Zemplèn conditions, affording the monovalent ligand **10** in 87% yield.

(25) Sabesan, S.; Neira, S. *Carbohydr. Res.* **1992**, *223*, 169−185.

(26) Mereyela, H. B.; Gurrala, S. R. *Carbohydr. Res.* **1998**, *307*, 351−354.

(27) Rostovtsev, V. V.; Green, L. G.; Fokin, V. V.; Sharpless, K. B. *Angew. Chem., Int. Ed.* **2002**, *41*, 2596−2599.

The same protocol was sucessfully repeated with polyazidosugars **2**−**7**. Yields ranged from 58 to 76% for the dipolar cycloaddition reaction (→ **11**, **13**, **15**, **17**, **19**, and **21**) and from 56 to 89% for the Zemplèn deprotection step (→ **12**, **14**, **16**, **18**, **20**, and **22**). The coupling reaction was clean, and total consumption of the starting substrates was observed in all cases, with formation of the expected cycloadducts as the only reaction products (Chart 2). The somewhat moderate isolation yields were probably due to partial protonation of the triazole ring over silica gel during purification. Furthermore, the reaction was found to be highly regioselective, yielding 1,4-disubstituted 1,2,3-triazole-containing pseudo-oligosaccharides. The olefinic proton associated with the triazole ring was identified as a singlet at $\delta = 7.5-8$ ppm. The large $\Delta(\delta_{C-4} - \delta_{C-5})$ values observed for the different triazoles, ranging from 19 to 25 ppm, corroborated the 1,4-disubstituted structure since much smaller values would be expected for 1,5-disubstituted regioisomers.[28]

The new glycococlusters prepared in this study display structural differences that are governed by the sugar scaffold substitution pattern as well as configurational and conformational biases, offering a good opportunity to test the influence of such factors on carbohydrate−protein recognition. The whole ligand set includes α-D-mannopyranosyl conjugates with valencies ranging from 1 to 4. Compounds exhibiting the same valency, such as **14**, **16** and **18**, or **20** and **22**, differ by the relative position of the mannosyl residues, one of them being attached at either a primary C-6 position or the anomeric position, in that case, with either an α- or β-configuration. As a suitable protein receptor model, the leguminous tetrameric lectin Con A, which specifically recognizes α-D-mannopyranosyl residues,[29] has been considered.

Affinity for Con A. The affinities of the prepared glycoconjugates toward Con A were evaluated by the ELISA-type protocol ELLA. This experiment measures the capacity of a soluble ligand to inhibit the lectin binding to a polymeric ligand that is used as a coating material on the microtiter well. In the present case, competitive experiments using horseradish peroxidase labeled Con A (HRP-Con A) as the lectin and yeast mannan as the microplate fixed ligand were carried out in triplicate. Methyl α-D-mannopyranoside was included in the tests as a reference compound. Up to eight different concentrations of each sample were considered, and the percentage of the inhibition of HRP-Con A−yeast mannan association was determined spectrophotometrically. The IC_{50} values (mean of three measurements), defined as the concentration of synthetic compound to achieve 50% inhibition of this association, were determined from the corresponding inhibition curves. IC_{50} values are assumed to be inversely proportional to the corresponding free energy of binding.

Binding affinities of the reference and synthetic glycoconjugates for Con A are summarized in Figure 1. The valency-corrected relative binding potencies expressed per mol of mannopyranosyl residue relative to the monovalent compound **10** ($IC_{50} = 267 \pm 28$ μM) are presented in Figure 2. The experimental data indicate that **10** is a 3-fold more efficient ligand for Con A as compared to methyl α-D-mannopyranoside. Similar affinity enhancements have been previously reported for aryl mannopyranosides.[30] On the basis of molecular modeling, NMR, and X-ray evidence, this effect has been ascribed to stabilizing interactions between aromatic aglycon and protein amino acids nearby once the mannopyranosyl residue is located in the binding site of Con A.[31] A similar scenario probably applies in the case of the aglyconic triazole ring.

The divalent derivative **12** exhibited a remarkable cluster effect. The binding efficiency was 6-fold higher as compared to monovalent **10**, which means 3-fold on a mannose molar basis. No precipitation was observed during the lectin binding assay at any concentration, supporting an aggregation independent mechanism.[32,33]

Previous results have shown that the presence of the peroxidase label used in ELLA actually promotes 1:1 sugar ligand/lectin stoichiometries.[34] Since the short distance between the binding epitopes, which cannot expand the distance between two recognition sites in Con A (about 65 Å), prevents a chelate binding mode, the important affinity enhancement observed must be ascribed to either the existence of an extended binding site in the lectin that can establish favorable interactions with both mannosyl residues simultaneously[35] or to a sliding mechanism between the two mannopyranosyl subunits in the maltosyl scaffold at the primary monosaccharide binding site in Con A.[36]

Going from divalent to trivalent arrangements (**14**, **16**, and **18**) led to higher affinities ($IC_{50} = 33 \pm 3$, 31 ± 3, and 33 ± 4 μM, respectively), although the per mannose binding efficiencies were slightly poorer (2.7−2.9). For the tetravalent glycoclusters **20** and **22**, we observed a similar trend, with binding affinities of 25 ± 3 and 23 ± 2 μM and valency-corrected affinities of 2.7 and 2.9. The incorporation of additional mannosyl units led, therefore, to merely statistical binding affinity enhancements. This result supports the occurrence of a sliding process that is optimal for the dimeric compound and suffers from enthalpy−entropy compensation for higher valent compounds. The existence of an extended binding site would

(28) Rodios, N. A. *J. Heterocycl. Chem.* **1984**, *21*, 1169−1173.

(29) (a) Bouckaert, J.; Hamelryck, T.; Wyns, L.; Loris, R. *Curr. Opin. Struct. Biol.* **2001**, *11*, 635−643. (b) Vijayan, M.; Chandra, N. *Curr. Opin. Struct. Biol.* **1999**, *9*, 707−714.

(30) (a) Iyer, R. N.; Goldstein, I. J. *Immunochemistry* **1973**, *10*, 313. (b) Van Wauve, J.-P.; Loontiens, F. G.; Carchon, H. A.; De Bruyne, C. K. *Carbohydr. Res.* **1973**, *30*, 249. (c) Loontiens, F. G.; Van Wauve, J.-P.; De Gussem, R.; De Bruyne, C. K. *Carbohydr. Res.* **1973**, *30*, 51. (d) Van Wauve, J.-P.; Loontiens, F. G.; De Bruyne, C. K. *Biochim. Biophys. Acta* **1975**, *379*, 456. (e) Pagé, D.; Zanini, D.; Roy, R. *Bioorg. Med. Chem.* **1996**, *4*, 1944−1961.

(31) (a) Hamodrakas, S. J.; Alexandraki, E.; Troganis, A.; Stassinopoulou, C. I. *Int. J. Biol. Macromol.* **1989**, *11*, 17−22. (b) Kanellopoulos, P.; Pavlou, K.; Perrakis, A.; Agianian, B.; Vorgias, C. E.; Mavrommatis, C.; Soufi, M.; Tucker, P. A.; Hamodrakas, S. *J. Struct. Biol.* **1996**, *116*, 345−355.

(32) Corbell, J. B.; Lundquist, J. J.; Toone, E. J. *Tetrahedron: Asymmetry* **2000**, *11*, 95−111.

(33) Formation of soluble aggregates between Con A and rigid oligomannosides has been observed. However, in solution, lectin recruitement should be reflected in activation, rather than inhibition, of the association of the lectin to the reference mannan fixed in the microplate well surface upon addition of the multi-valent ligands, resulting in abnormal inhibition curves, which was not the present case. See: (a) Burke, S. D.; Zhao, Q.; Schuster, C.; Kiessling, L. L. *J. Am. Chem. Soc.* **2000**, *122*, 4518−4519. (b) Gestwicki, J. E.; Cairo, C. W.; Strong, L. E.; Oetjen, K. A.; Kiessling, L. L. *J. Am. Chem. Soc.* **2002**, *124*, 14922−14933.

(34) Gómez-García, M.; Benito, J. M.; Rodríguez-Lucena, D.; Yu, J.-X.; Chmurski, K.; Ortiz Mellet, C.; Gutiérrez Gallego, R.; Maestre, A.; Defaye, J.; García Fernández, J. M. *J. Am. Chem. Soc.* **2005**, *127*, 7970−7971.

(35) Con A is known to possess an extended binding site for the Man*p*-a(1 → 3)-[Man*p*-a(1 → 6)]-Man trisaccharide core. See: (a) Mandal, D. K.; Battachariyya, L.; Koening, S. H.; Brown, R. D., III; Oscarson, S.; Brewer, C. F. *Biochemistry* **1994**, *33*, 1157. (b) Weatherman, R. V.; Mortell, K. H.; Chervenak, M.; Kiessling, L. L.; Toone, E. J. *Biochemistry* **1996**, *35*, 3619−3624.

(36) Dam, T. K.; Brewer, C. F. *Chem. Rev.* **2002**, *102*, 387−429.

CHART 2. Structure (Isolated Yield) of Glycoclusters 11−22

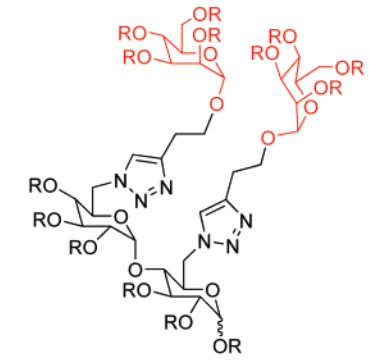

11 R=OAc 66%
12 R=H 56%

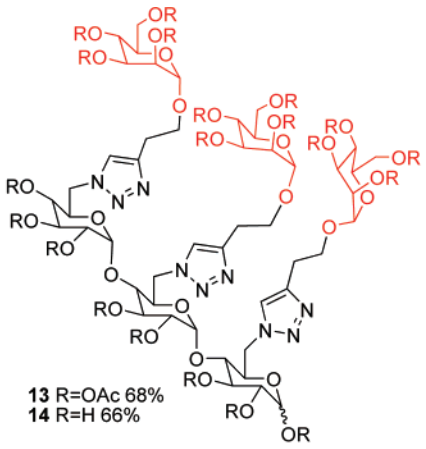

13 R=OAc 68%
14 R=H 66%

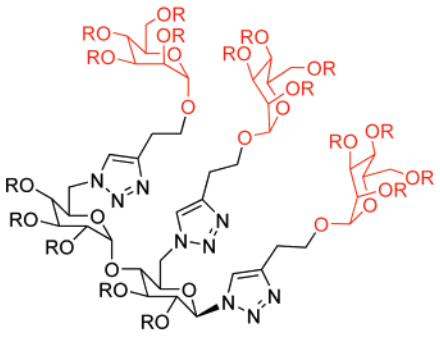

15 R=OAc 76%
16 R=H 77%

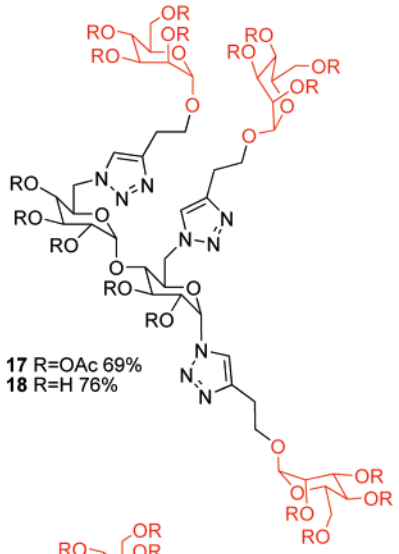

17 R=OAc 69%
18 R=H 76%

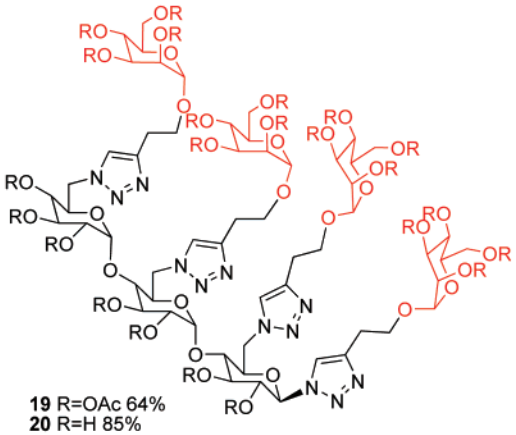

19 R=OAc 64%
20 R=H 85%

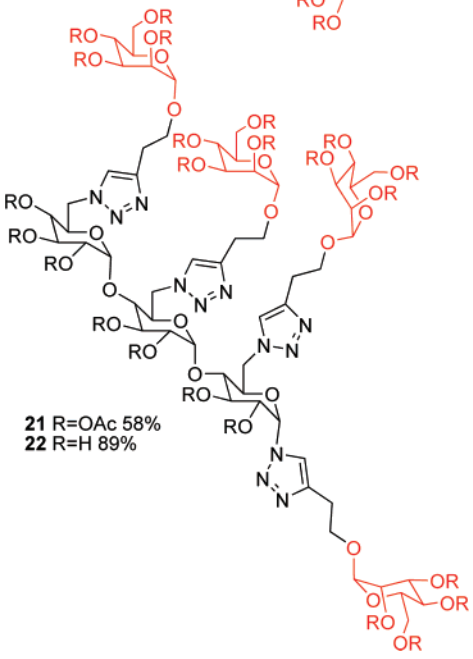

21 R=OAc 58%
22 R=H 89%

be expected to be translated into a significant decrease in relative binding affinity with valency unless the critical fragment is repeated.

No significant differences were observed for trivalent and tetravalent ligands with regards to the spatial arrangement of the epitopes. For trimannosides (**14**, **16**, and **18**), the binding

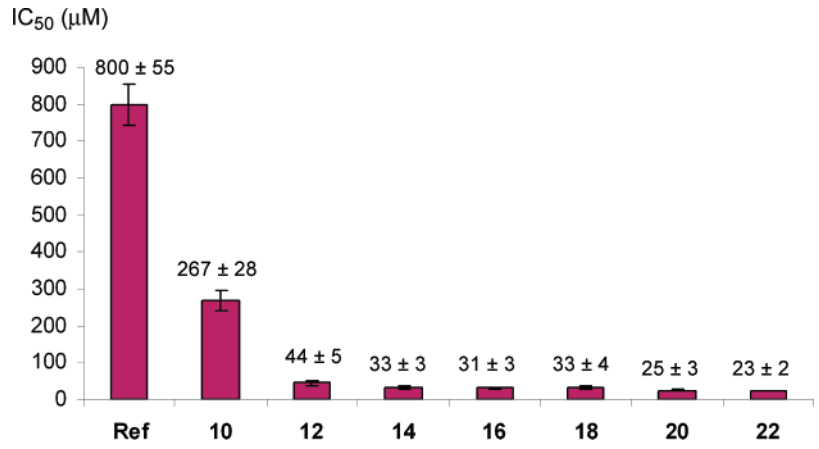

FIGURE 1. Binding affinities of methyl mannoside (ref) and synthetic glycoclusters for Con A.

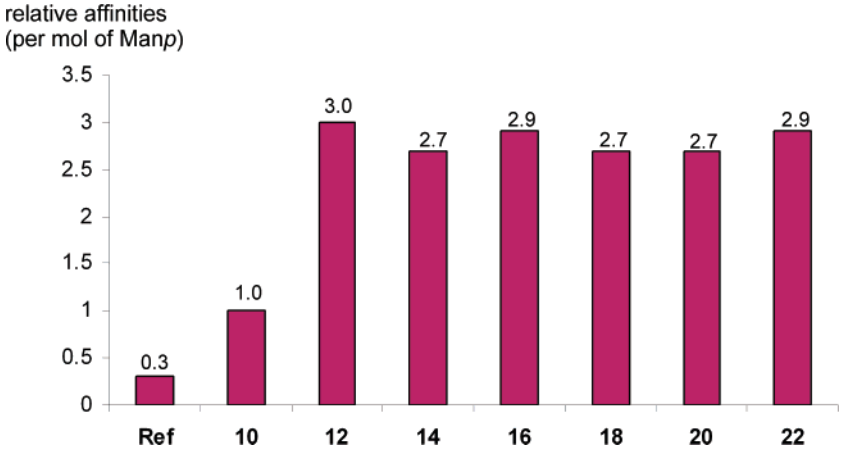

FIGURE 2. Valency-corrected relative binding potency (per mol of mannopyranoside residue).

affinity remains virtually unchanged when a mannopyranosyl substituent is switched from the C-6 to the anomeric position, irrespective of the α- or *β*-anomeric configuration. Analogously, the α- and *β*-tetravalent glycolusters **20** and **22** exhibited comparable binding affinities.

Force Field Development and Atom Charge Value Derivation. Molecular simulations were carried out using the Glycam 2004 force field.[37] However, in the absence of force field topological fragments and RESP atom charge values for triazole derivatives in this force field,[38] a new force field topology database (FFTPDB) compatible with glycoclusters **10**, **12**, **14**, **16**, **18**, **20**, and **22**, and more generally with any Glc-α-(1 → 4)-based polymer, was developed. Multiple molecules, multiple conformations, and multiple molecular orientations were used in charge derivation. A detailed description of this procedure is reported in the Experimental Section. Five molecules, namely, α- and *β*-D-glucopyranose, methyl α-D-glucopyranoside, methyl α-D-mannopyranoside, and 1-*N*-methyl-4-(2-hydroxyethyl)-1,2,3-triazole, were considered (Scheme 3A). Two conformations with the *ω* dihedral angle about the C5′−C6′ bond corresponding to gauche, gauche (*gg*) and gauche, trans (*gt*) conformations were selected for the glucose and mannose derivatives since these conformations are the most commonly observed in solution for these two monosaccharides.[39] In the absence of experimental data for 1-*N*-methyl-4-(2-hydroxyethyl)-1,2,3-triazole, the two lowest minima observed after geometry optimization were chosen. Optimized geometries presenting intra-molecular hydrogen bonds were not used in the charge derivation to avoid an over-polarization effect. This approach is compatible with the use of implicit polarization in AMBER and GLYCAM force fields.[38a,40] Four molecular orientations for each optimized geometry were generated before molecular electrostatic potential (MEP) computation and were involved in the charge fitting procedure to yield reproducible atom charge values.[41] Inter-molecular charge constraints between methyl and hydroxyl groups were used in charge fitting, allowing the definition of the required molecular fragments (Scheme 3A,B). The charge value of each hydrogen bound to a carbon presenting sp^3 hybridization was set to a constrained value of zero to ensure a compatibility between this work and the GLYCAM 2004 force field.[42]

(37) (a) Kirschner, K. N.; Woods, R. J. *J. Phys. Chem. A* **2001**, *105*, 4150−4155. (b) Basma, M.; Sundara, S.; Calgan, D.; Varnali, T.; Woods, R. J. *J. Comput. Chem.* **2001**, *22*, 1125−1137. (c) Kirschner, K. N.; Woods, R. J. *Proc. Natl. Acad. Sci. U.S.A.* **2001**, *98*, 10541−10545.

(38) (a) Bayly, C. I.; Cieplak, P.; Cornell, W. D.; Kollman, P. A. *J. Chem. Phys.* **1993**, *97*, 10269−10280. (b) Woods, R. J.; Chappelle, R. *J. Mol. Struct.* **2000**, *527*, 149−156.

(39) (a) Marchessault, R. H.; Perez, S. *Biopolymers* **1979**, *18*, 2369−2374. (b) Bock, K.; Duus, J. O. *J. Carb. Chem.* **1994**, *13*, 513−543.

(40) Cornell, W. D.; Cieplak, P.; Kollman, P. A. *J. Am. Chem. Soc.* **1993**, *115*, 9620−9631.

(41) Pigache, A.; Cieplak, P.; Dupradeau, F.-Y. *Automatic and Highly Reproducible RESP and ESP Charge Derivation: Application to the Development of Programs RED and X RED*, 227th ACS National Meeting, Anaheim, CA, March 28 to April 1, 2004; ACS: Washington, DC, 2004.

SCHEME 3. FFTPDB Constructed Using α- and β-D-Glucopyranose, Methyl α-D-Glucopyranoside, Methyl α-D-Mannopyranoside, and 1-*N*-Methyl-4-(2-hydroxyethyl)-1,2,3-triazole[a]

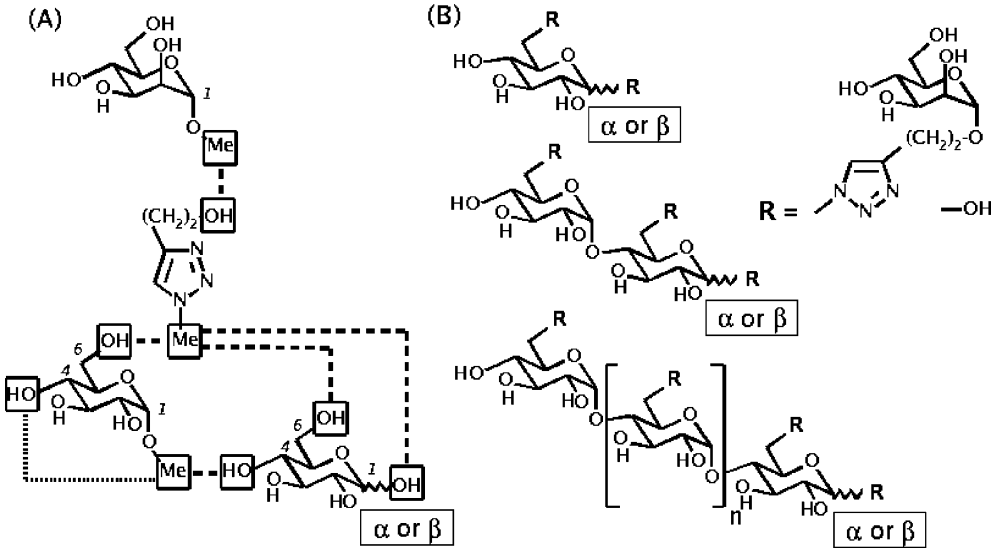

[a] (A) Inter-molecular (represented by a dashed line) and intra-molecular (represented by a fine dashed line) charge constraints between methyl (belonging to methyl α-D-glucopyranoside, methyl α-D-mannopyranoside, and 1-*N*-methyl-4-(2-hydroxyethyl)-1,2,3-triazole) and hydroxyl boxed groups (belonging to methyl α-D-glucopyranoside, methyl α-D-mannopyranoside, and 1-*N*-methyl-4-(2-hydroxyethyl)-1,2,3-triazole) were used in charge fitting. (B) Glycoclusters **10**, **12**, **14**, **16**, **18**, **20**, and **22** and polymeric Glc-α-(1 → 4)-based oligosaccharides were built using this new FFTPDB.

Validation of the FFTPDB. This work represents the first description of the FFTPDB reported. To check the validity of this FFTPDB and in the absence of experimental data for the ligands studied, and of triazol derivative units in the Glycam 2004 force field, a comparative study involving the glucose scaffold [disaccharide Glc-α-(1 → 4) α-Glc] was carried out using the molecular fragments and charge values taken from the Glycam 2004 force field and the FFTPDB described in this work. MD simulations were carried out for 10 ns, in presence of explicit water molecules, and MD snapshots were generated every 2 ns. Comparison of these MD snapshots reveals highly similar three-dimensional structural features (Figure S1). Heavy atom rmsd between the 10 MD snapshots selected and the average structure of these snapshots present a maximum rmsd values of 1.0 Å. This shows the excellent agreement of the structures obtained using the two approaches and the establishment of a well-defined family of three-dimensional structures for the glucose-based disaccharide. Indeed, in both computational conditions, two persistent inter-unit hydrogen bonds (H-bonds) were observed during MD between the hydroxyl 3 of the reductive unit and the hydroxyl 2 of the second glucose unit, each oxygen atom taking successively the role of the acceptor or donor of the H-bond. These inter-glucose H-bonds participate in the formation of stable structures for the glucose scaffold. To further validate our FFTPDB, the evolution of the ω dihedral angle values for the two glucose units was followed during MD simulations. Oscillating values corresponding to *gt* and *gg* rotamers (Figures S2A−D) were observed in both computational conditions, which is consistent with experimental data.[39] Thus taken all together, the results obtained in this comparative study unambiguously demonstrate the validity of the FFTPDB reported.

MD Simulation. Structures of glycoclusters **12**β, **12**α, **16**, and **18** were studied during 10 ns of MD simulation in the presence of explicit water molecules. Highly similar structural features were observed for the different glycoclusters studied. As an illustrative example, the survey for glycocluster **18** is discussed herein. The presence of H-bonds, which reflects the formation of a putative stable structure during the simulation, was first checked. The 10 most frequent H-bonds observed are reported in Table 1. A single stable H-bond between the HO3′−O3′ donor of glucose unit 2 and the O2′ acceptor of glucose unit 1 was detected, demonstrating the absence of a well-defined three-dimensional structure for glycocluster **18**. It is worth noting that this H-bond was already observed in the disaccharide Glc-α-(1 → 4) α-Glc simulation. This demonstrates the reproducibility of the results obtained using different models and validates the FFTPDB described. On the contrary, several transient H-bonds were observed during the simulation defining different local minima.

The Φ (O5′−C1′−O1′−C4′), ψ (C1′−O1′−C4′−C3′), and ω dihedral angles of the glucose and mannose units of glycocluster **18** were followed during MD simulation. The values of those dihedral angles are reported in Figure S3 (see Supporting Information). The ω dihedral angle about the C5′−C6′ bond of the glucose scaffold units exhibited striking constant values corresponding to the *gt* population (Figure S3A,B). This result is explained by the establishment of specific stabilizing interactions within the glycocluster. Indeed, nonclassical H-bond

(42) RRMS (relative root mean square value between MEP calculated by quantum mechanics and that generated using the derived charge values) of 0.126 was obtained for the fit. Intra-molecular charge constraints, inter-molecular charge constraints, charge value equivalencing between the different molecular orientations and conformations, and the hyperbolic constraint of the restrained fit are accountable for an increase of 0.005, 0.003, 0.010, and 0.006 of the RRMS value, respectively. These values rigorously demonstrate the strength and weakness of the approach followed. The RESP charge derivation procedure was automatically carried out using the RESP ESP charge Derive (R.E.D.) program (http://q4md-forcefield-tools.org/RED/).[41] The RESP atom charge values and FFTPDB were submitted in the RESP ESP charge DDataBase (R.E.DD.B.) (http://q4md-forcefieldtools.org/REDDB/) and are available as the "F-71" R.E.DD.B. project code as a suite of files in the Tripos mol2 file format considered as force field library precursors (http://www.tripos.com/index.php?family=modules,-SimplePage,,,&page=sup_mol2&s=0).

TABLE 1. Ten Most Frequent H-Bonds Detected during 10 ns MD Simulation for Glycocluster 18[a]

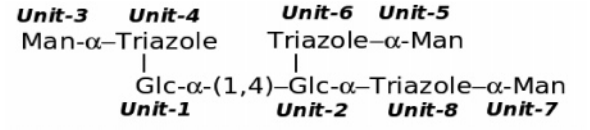

H-bond acceptors	H-bond donors	% of occupancy during the simulation
1:O2'	2:HO3' 2:O3'	|++--+-+---|
6:N4	3:HO4' 3:O4'	| - o +|
2:O3'	5:HO3' 5:O3'	| - +-o |
1:O3'	3:HO3' 3:O3'	| +o |
6:N5	3:HO4' 3:O4'	| o -|
6:N4	3:HO6' 3:O6'	| -- |
2:O3'	1:HO2' 1:O2'	| - |
2:O3'	5:HO4' 5:O4'	| -- |
6:N4	5:HO6' 5:O6'	| - - |
5:O4'	7:HO4' 7:O4'	| + |

[a] Loose H-bond criteria [distance (acceptor−donor) = 3.2 Å (3.0 is the canonical value) and angle (acceptor−hydrogen−donor) = 120° (180 is the canonical value)] were selected for H-bond printing ensuring the detection of both weak and strong H-bonds. Notation of H-bond acceptors and donors corresponds to "unit number:atom name". For the schematic representation of the percentage of occupancy observed during the simulation, the following convention has been used: "blank", >0−5%; "−", 5−20%; "+", 20−40%; and "o", 40−60%. For notation of the triazole atom numbers, see the Supporting Information.

interactions were detected between the endocyclic O5′ oxygen of glucose unit 1 or 2 and the H7 proton at the triazole unit 4 or 6 (Figure S4A−C). Although weak, the nonbonding interaction involving the H7 atom of unit triazole derivative 6 is unequivocal. Indeed, this atom unambiguously interacts with the O5′ acceptor of units glucose 1 or 2, after rotation around the O5′−C5′−C6′−N6 dihedral angle (Figure S4B,C). To further substantiate this result, model structures were optimized in the gas phase by ab initio calculations using the B3LYP/6-311+G** theory level,[43] and an optimal distance of 2.75 Å was found between the H7 and the O5′ atoms for the lowest minimum. On the contrary, ω dihedral angles for the three mannose units oscillated between values corresponding to the expected *gt* and *gg* rotamers (Figure S3C−E), which is consistent with experimental data.[39] This observation is another argument in favor of the validity of the FFTPDB reported. It is important to emphasize that the HO6′ hydroxyl of mannose units 3, 5, and 7 remained solvated during most of the simulation time, preventing the formation of stable intra-glycocluster interactions involving this primary hydroxyl group. Finally, the Φ and ψ dihedral angles displayed similar values during MD simulation (Figure S3F−K), corresponding to gauche populations. This result is a strong argument in favor of the adoption of a stable structure for the glucose scaffold. In particular, the dihedral angle ψ observed in glycocluster **18** within the glucose scaffold was stabilized by the H-bond interaction previously reported between the HO3′−O3′ donor of glucose unit 2 and the O2′ acceptors of glucose unit 1 (Table 1).

As compared to the Φ, ψ, and ω dihedral angles of the glucose and mannose units, the dihedral angles involving the triazole derivative units display strikingly different features. Similar dihedral profiles were observed during the simulation for triazole units 4, 6, and 8 during the simulation. Consequently, only the study of the dihedral angle values for unit 4 is presented in Figure S5A−D as a demonstration. The C5′−C6′−N6−N5 dihedral angles between units 1 and 4 display similar values during the simulation (Figure S5A). This provides new evidence for the inter-unit interaction previously described involving the H7 hydrogen and O5′ endocyclic oxygen of triazole derivative units 4 and glucose 1, respectively. On the contrary, the three other dihedral angles studied involving the triazole derivative units 4 and mannose 3 (C1′−O1′−C1−C2, O1′−C1−C2−C3, and C1−C2−C3−N4) display highly variable values (Figure S5B−D). This observation is in agreement with the presence of different local minima reflecting an important flexibility in this region of glycocluster **18**. The repetition of such dihedral profiles for the three triazole derivative units led to the formation of disorganized three-dimensional structures for glycocluster **18** allowing each mannose unit to adopt different orientations. To further characterize this result, MD snapshots were selected every nanosecond and superimposed over the last structure using the pyranose ring atoms belonging to the glucose scaffold. Figure 3 presents three-dimensional structures of glycoclusters **12*β***, **12α**, **16**, and **18** generated using this approach. This clearly demonstrates the definition of regions with different dynamic behaviors for each glycocluster. Indeed, independently of the glycocluster studied, a rigid and well-defined domain for the glucose scaffold and highly flexible counterparts composed of the mannose units are observed. Two stabilizing forces were clearly identified within the glycoclusters that participate in the definition of the characteristic glucose scaffold structure. The first one is a H-bond between hydroxyl 3 of the glucose unit of the reductive side and hydroxyl 2 belonging to the other glucose unit. The second one is a nonbonding interaction between the endocyclic O5′ oxygen of glucose unit 1 or 2 and the C7−H7 hydrogen belonging to the triazole ring of unit 4 or 6. Moreover, the role of the ethylene segments connecting the mannopyranosyl substituents and the triazole rings is central to the high flexibility observed. It is particularly striking for glycoclusters **16** and **18**. Indeed, although the spatial arrangements for α- and β-anomers are different, each ligand being located on opposite faces of the scaffold plan, similar ELLA data are obtained for these two glycoclusters. This clearly shows the importance of the ethylene groups in the glycocluster building strategy, and their central role in the flexibility and ELLA results is observed. On the other hand, the MD simulations performed for **16** and **18** indicated that the rigidity of the maltosyl scaffold virtually prevented conformations from having simultaneously the three mannose residues in close spatial proximity, while conformations having two of them in the same region are frequent. This dynamic behavior probably explains the high cluster effect observed for divalent compounds. While sliding of the lectin between two vicinal mannnosyl ligands is strongly favored, moving along the maltooligosaccharide scaffold to the next mannosyl pair has a penalty associated with the adoption of transient unfavorable conformations. Thus, the results are compatible with the existence of a sliding mechanism that would be optimal for the divalent compound that undergoes enthalpy−entropy compensation for the tri- and tetravalent derivatives at the origin depending on the structures. The loss of entropy when the mannose binds to the lectin is compensated by a gain of

(43) Hehre, W. J.; Radom, L.; Schleyer, P. v. R.; Pople, J. A. *Ab Initio Molecular Orbital Theory*; John Wiley and Sons: New York, 1986.

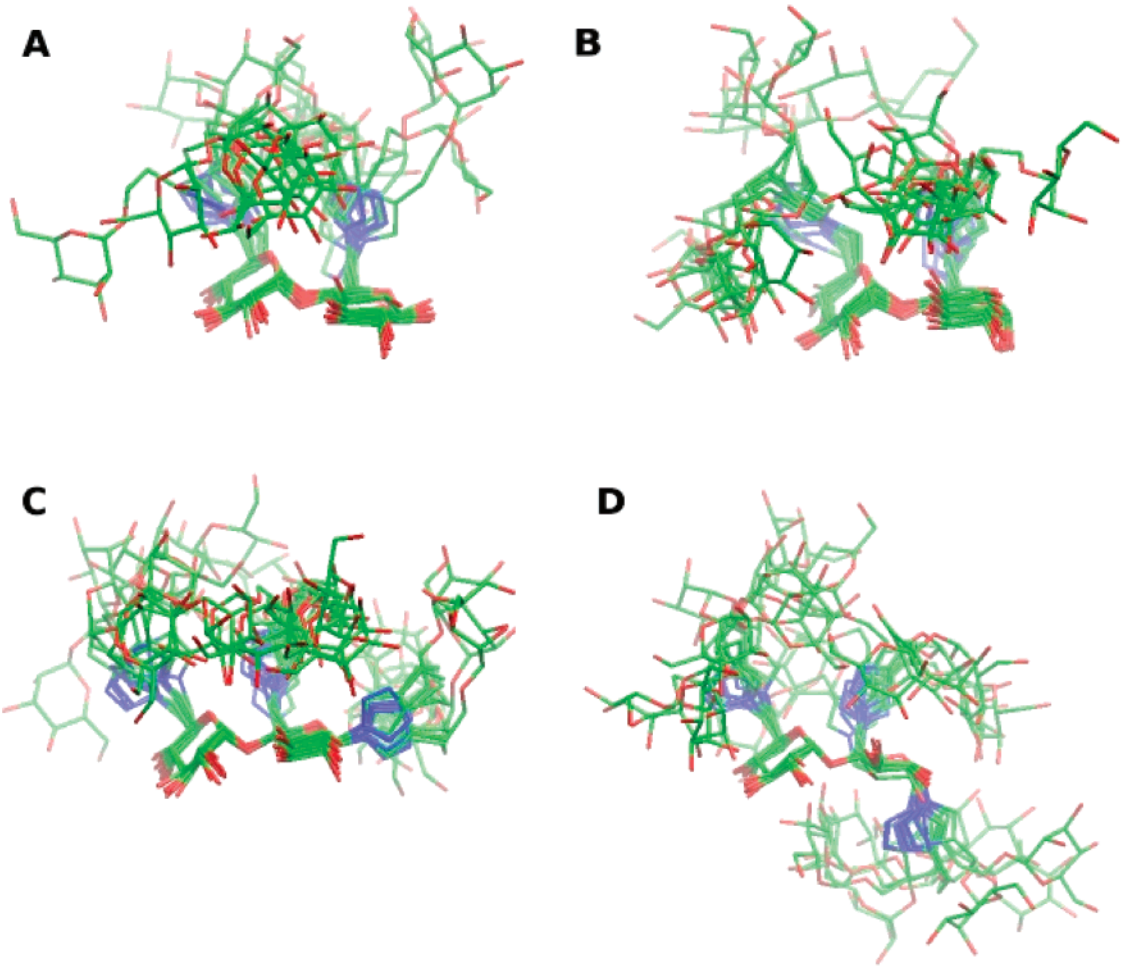

FIGURE 3. Three-dimensional structures of glycoclusters **12*β***, **12α**, **16**, and **18** observed during 10 ns MD simulation. For each glycocluster, MD snapshots were selected every nanosecond, superimposed over the last structure using the pyranose ring atoms of the glucose scaffold, and displayed (hydrogen atoms are not represented for clarity). (A) Structures of glycocluster **12*β***; (B) structures of glycocluster **12α**; (C) structures of glycocluster **16**; and (D) structures of glycocluster **18**.

enthalpy resulting from the establishment of specific electrostatic interactions between the ligand and the protein within the binding site.

It is noteworthy that previous work using mannosyl coated flexible dendritic cores had shown optimal affinity enhancements for α-D-mannopyranosyl triads, while divalent compounds exhibited relative binding affinities lower than the monovalent counterparts.[44] The present results underline the importance of the scaffold architecture on the lectin binding affinity properties of multi-valent glycoligands. A fine, mechanism-based tuning of carbohydrate−lectin interactions can be achieved by controlling the distance between the binding epitopes, their relative spatial orientation, and the dynamic behavior of the whole system.

Conclusion

In summary, we described in this paper a short and efficient strategy for the synthesis of carbohydrate-centered multi-mannosides using click chemistry. Regioselective azidation of unprotected commercial mono- and oligosaccharides with triphenylphosphine-carbon tetrabromide-sodium azide allows the requested polyazido templates to be accessed in one pot. In addition, we have shown that the degree of azidation can be modulated by acting on the reagent ratio. Further coating with a model alkynyl mannoside by click chemistry proceeded cleanly to give the target polyconjugates. Evaluation of the binding affinity against Con A lectin by ELLA indicated the existence of stabilizing interactions between the generated 1,2,3-triazole ring and the protein for a monovalent derivative. Interestingly, higher valent compounds exhibited strong and comparable cluster effects (molar relative potencies ranging from 8.1 to 9.1), irrespective of valence (2−4) or spatial arrangement. The results are compatible with the existence of a sliding mechanism that would be optimal for the divalent compound and undergoes enthalpy−entropy compensation for the tri- and tetravalent derivatives. MD calculations performed on representative glycoconjugates indicated that these compounds combine a remarkable rigidity of the oligosaccharide scaffold and a relatively high flexibility of the mannosyl branches that is consistent with the ELLA observations. The possibility of modulating the orientational properties and dynamic behavior in multi-valent glycoligands based on regioselectively func-

(44) Baussanne, I.; Benito, J. M.; Ortiz Mellet, C.; García Fernández, J. M.; Law, H.; Defaye, J. *Chem. Commun.* **2000**, 1489−1490.

tionalized carbohydrate scaffolds makes these conjugates promising tools as probes or effectors of biological processes.

Experimental Section

General Procedure for the Synthesis of Azido Compounds. Carbohydrate (1.38 mmol of monosaccharide unit) and sodium azide (0.903 or 1.801 g, 13.9 or 27.7 mmol) were dissolved in anhydrous DMF (8 mL) at room temperature (rt). PPh_3 (0.726 or 1.456 g, 2.77 or 5.55 mmol) was added to the mixture, and after 30 s of stirring, CBr_4 (0.919 or 1.841 g, 2.77− or 5.55 mmol) dissolved in anhydrous DMF (2 or 4 mL) was added dropwise (slight exotherm was observed). The resulting mixture was stirred at rt for 60 h under nitrogen. Methanol (5 mL) was added, and the solution was filtered. After evaporation under reduced pressure, water (20 mL) and toluene (20 mL) were added. The mixture was vigorously stirred, and ethyl acetate was added dropwise until the system became clear. The organic layer was extracted with water (3 × 20 mL). Aqueous layers were combined, and the solution was evaporated under vacuum. The dry residue was dissolved in 1:1 Pyr/Ac_2O (50 mL). After 12 h at rt, the solvent was removed under reduced pressure, and the residue was dissolved in ethyl acetate (20 mL). The organic layer was washed with water (20 mL), dried over Na_2SO_4, filtered, and evaporated to dryness. The residue was purified by flash chromatography (FC) (cyclohexane/ethyl acetate or toluene/diethyl ether) leading to azido compounds.

General Procedure for the Click Reaction. Compounds **9**, **11**, **13**, **15**, **17**, **19**, and **21** were synthesized using this procedure. Alkynyl-saccharide **8** (152 mg, 0.38 mmol) and azido-saccharide **4** (80 mg, 0.13 mmol) were dissolved in a DMF/H_2O mixture (8:2 mL). Copper sulfate (0.19 mmol) and sodium ascorbate (0.38 mmol) were added, and the mixture was stirred at rt until MS indicated the disappearance of starting materials and intermediates (10−16 h). The mixture was poured into a 1:1 H_2O/NH_4Cl saturated solution (60 mL) and extracted with EtOAc (4 × 30 mL). The organic layer was dried over Na_2SO_4 and filtered, and the solvent was removed under reduced pressure. The residue was purified by flash chromatography to give **15** (177 mg, 76% yield).

General Procedure for Deacetylation. Compounds **10**, **12**, **14**, **16**, **18**, **20**, and **22** were synthesized using this procedure. The cycloadduct (70 mg) was dissolved in dry MeOH (4 mL). A solution of sodium methanolate (1 M) in methanol (133 μL) was added, and the mixture was stirred under N_2 at rt until MS indicated the total disappearance of starting materials and intermediates (3 h). In some cases, precipitation of the product occurred. If so, water was added until complete dissolution of the precipitate. Amberlyst IR120(H^+) was added, and the mixture was stirred until the pH reached 5. The resin was filtered off, and the solution was evaporated to dryness leading to the pure unprotected product.

2,3,4-Tri-*O*-acetyl-6-azido-6-deoxy-α-D-glucopyranosyl-(1 → 4)-1,2,3-tri-*O*-acetyl-6-azido-6-deoxy-D-GLUCOPYRANOSE (2). ^{1}H NMR (300 MHz, $CDCl_3$) Δ = 6.26 (1H, D, $J_{1,2}$ 3.8 Hz, *H*-1A), 5.72 (1H, D, $J_{1,2}$ 8.1 Hz, *H*-1B), 5.50−5.28 (6H, M, *H*-3AB, *H*-1′AB, *H*-3′AB), 5.01 (4 H, M, *H*-2AB, *H*-4′AB), 4.82 (2H, M, *H*-2′AB), 4.12 (4H, M, *H*-4AB, *H*-5AB), 3.81 (2H, M, *H*-5′AB), 3.67 (2H, M, *H*-6AAB), 3.42 (5H, M, *H*-6BAB, *H*-6′AAB, *H*-6′BB), 3.29 (1H, DD, $J_{5',6'B}$ 5.0 Hz, $J_{6'A,6'B}$ 13.4 Hz, *H*-6′BA), 2.18, 2.03, 2.02, 2.01, 1.98, 1.96, 1.95 (36H, 7S, 12 × C*H*$_3$CO); ^{13}C NMR (75 MHz, $CDCL_3$): Δ = 170.5, 170.2, 170.1, 169.8, 169.5, 169.0 (*C*O), 95.4 (*C*-1′A), 95.2 (*C*-1′B), 91.4 (*C*-1B), 88.9 (*C*-1A), 76.7, 75.1, 74.3, 73.9, 72.1, 71.7, 71.5, 71.0, 69.8, 69.7, 69.3, 69.1 (*C*-2 TO *C*-5AB, *C*-2′ TO *C*-5′AB,), 51.0, 50.8, 50.7 (*C*-6AB, *C*-6′AB), 21.0, 20.8, 20.7, 20.6, 20.5 (*C*H$_3$CO); HRMS (ES+): FOUND 667.1834 $C_{24}H_{32}N_6O_{15}Na$ REQUIRES 667.1823 [M + Na^+].

2,3,4-Tri-*O*-acetyl-6-azido-6-deoxy-α-D-glucopyranosyl-(1 → 4)-2,3-di-*O*-acetyl-6-azido-6-deoxy-α-D-glucopyranosyl Azide (3). [α]$^{20}_D$ +162 (*c* 0.1, CH_2Cl_2); ^{1}H NMR (300 MHz, $CDCl_3$) δ = 5.56 (1H, d, $J_{1,2}$ 4.2 Hz, *H*-1), 5.46−5.40 (2H, m, *H*-3, *H*-1′), 5.31 (1H, t, $J_{2',3'} = J_{3',4'}$ 10.0 Hz, *H*-3′), 5.01 (1H, t, $J_{3',4'} = J_{4',5'}$ 9.6 Hz, *H*-4′), 4.83 (1H, dd, $J_{2,3}$ 10.0 Hz, *H*-2), 4.83 (1H, dd, $J_{1',2'}$ 3.9 Hz, $J_{2',3'}$ 10.4 Hz, *H*-2′), 4.16−4.05 (2H, m, *H*-4, *H*-5), 3.84 (1H, m, *H*-5′), 3.70 (1H, dd, $J_{5,6a}$ 2.3 Hz, $J_{6a,6b}$ 11.7 Hz, *H*-6a), 3.52−3.46 (2H, m, *H*-6b, *H*-6′a), 3.33 (1H, dd, $J_{5,6'b}$ 5.0 Hz, $J_{6'a,6'b}$ 13.5 Hz, *H*-6′b), 2.06, 2.03, 1.99 (15H, 3s, 5 × C*H*$_3$CO); ^{13}C NMR (75 MHz, $CDCl_3$): δ = 170.5, 170.0, 169.9, 169.5 (*C*O), 95.2 (*C*-1′α), 86.2 (*C*-1α), 71.7, 71.4 (*C*-3, *C*-4, *C*-5), 70.6, 70.0(*C*-2, *C*-2′), 69.6 (*C*-4′), 69.2, 69.0 (*C*-3′, *C*-5′), 50.9 (*C*-6, *C*-6′), 20.9, 20.6, 20.5 (*C*H$_3$). HRMS (ES+): Found 650.1753 $C_{22}H_{29}N_9O_{13}Na$ requires 650.1783 [M + Na^+].

2,3,4-Tri-*O*-acetyl-6-azido-6-deoxy-α-D-glucopyranosyl-(1 → 4)-2,3-di-*O*-acetyl-6-azido-6-deoxy-β-D-glucopyranosyl Azide (4). [α]$^{20}_D$ +79 (*c* 0.1, CH_2Cl_2); ^{1}H NMR (300 MHz, $CDCl_3$) δ = 5.40 (1H, d, $J_{1',2'}$ 3.9 Hz, *H*-1′), 5.30 (1H, t, $J_{2,3} = J_{3,4}$ 9.8 Hz, *H*-3), 5.26 (1H, t, $J_{2',3'} = J_{3',4'}$ 9.6 Hz, *H*-3′), 4.97 (1H, t, $J_{3',4'} = J_{4',5'}$ 9.6 Hz, *H*-4′), 4.84−4.76 (2H, m, *H*-2′, *H*-2), 4.66 (1H, d, $J_{1,2}$ 8.8 Hz, *H*-1), 4.07 (1H, t, $J'_{,4} = J_{4,5}$ 9.8 Hz, *H*-4), 3.81−3.69 (3H, m, *H*-5, *H*-5′, *H*-6′a), 3.50−3.41 (2H, m, *H*-6a, *H*-6′b), 3.33 (1H, dd, $J_{5,6b}$ 5.0 Hz, $J_{6a,6b}$ 13.5 Hz, *H*-6b), 2.03, 2.02, 1.98 (15H, 3s, 5 × C*H*$_3$-CO); ^{13}C NMR (75 MHz, $CDCl_3$): δ = 170.4, 170.2, 170.0, 169.5, 169.4 (*C*O), 95.2 (*C*-1′), 87.5 (*C*-1), 76.2, 74.6, 71.5, 71.4, 70.1, 69.6, 69.1, 68.9 (*C*-2 to *C*-5, *C*-2′ to *C*-5′), 50.9 (*C*-6, *C*-6′), 20.8, 20.7, 20.6, 20.5 (*C*H$_3$CO). HRMS (ES+): Found 650.1813 $C_{22}H_{29}N_9O_{13}Na$ requires 650.1783 [M + Na^+].

2,3,4-Tri-*O*-acetyl-6-azido-6-deoxy-α-D-glucopyranosyl-(1 → 4)-2,3-di-*O*-acetyl-6-azido-6-deoxy-α-D-glucopyranosyl-(1 → 4)-1,2,3-tri-*O*-acetyl-6-azido-6-deoxy-D-glucopyranose (5). ^{1}H NMR (300 MHz, $CDCl_3$) δ = 6.23 (1H, d, $J_{1\alpha,2\alpha}$ 3.7 Hz, *H*-1α), 5.68 (1H, d, $J_{1,2}$ 8.1 Hz, *H*-1β), 5.50−5.23 (10H, m, *H*-3αβ, *H*-1′αβ, *H*-3′αβ, *H*-1″αβ, *H*-3″αβ), 4.95−4.90 (4H, m, *H*-2αβ, *H*-4″αβ), 4.77−4.65 (4H, m *H*-2′αβ, *H*-2″αβ), 4.08−3.90 (6H, m, *H*-4αβ, *H*-5αβ, *H*-4′αβ), 3.80−3.60 (8H, m, *H*-6aαβ, *H*-5′αβ, *H*-6′aαβ, *H*-5″αβ), 3.45−3.4 (6H, m, *H*-6bαβ, *H*-6′bαβ, *H*-6″aαβ), 3.25−3.22 (m, 2H, *H*-6″bαβ), 1.99, 1.98, 1.97, 1.95, 1.94, 1.93, 1.92 (48H, 7s, 16 × C*H*$_3$CO); ^{13}C NMR (75 MHz, $CDCl_3$): δ = 170.5, 170.1, 169.8, 169.7, 169.4, 168.9 (*C*O), 95.4, 95.3 (*C*-1′α, *C*-1″α, *C*-1′β, *C*-1″β), 91.2 (*C*-1β), 88.8 (*C*-1α), 75.0, 74.0, 72.0, 71.6, 71.4, 71.2, 70.9, 70.5, 70.3, 70.0, 69.7, 69.4, 69.1 (*C*-2 to *C*-5αβ, *C*-2′ to *C*-5′αβ, *C*-2″ to *C*-5″αβ), 50.8 (*C*-6, *C*-6′, *C*-6″αβ), 20.9, 20.8, 20.6, 20.5 (*C*H$_3$CO); HRMS (ES+): Found 938.2662 $C_{34}H_{45}N_9O_{21}Na$ requires 938.2628 [M + Na^+].

2,3,4-Tri-*O*-acetyl-6-azido-6-deoxy-α-D-glucopyranosyl-(1 → 4)-2,3-di-*O*-acetyl-6-azido-6-deoxy-α-D-glucopyranosyl-(11 → 4)-2,3-di-*O*-acetyl-6-azido-6-deoxy-α-D-glucopyranosyl Azide (6). [α]$^{20}_D$ +155 (*c* 0.7, CH_2Cl_2); ^{1}H NMR (300 MHz, $CDCl_3$) δ = 5.56 (1H, d, $J_{1,2}$ 4.2 Hz, *H*-1), 5.43−5.29 (5H, m, *H*-3, *H*-1′, *H*-3′, *H*-1″, *H*-3″), 5.00 (1H, t, $J_{3'',4''} = J_{4'',5''}$ 9.4 Hz, *H*-4″), 4.84 (1H, dd, $J_{1,2}$ 4.2 Hz, $J_{2,3}$ 10.0 Hz, *H*-2), 4.82 (1H, dd, $J_{1'',2''}$ 4.4 Hz, $J_{2'',3''}$ 10.0 Hz, *H*-2″), 4.73 (1H, dd, $J_{1',2'}$ 4.4 Hz, $J_{2',3'}$ 10.1 Hz, *H*-2′), 4.17−4.15 (1H, m, *H*-5), 4.09 (1H, t, $J_{3,4} = J_{4,5}$ 9.0 Hz, *H*-4), 4.07 (1H, t, $J_{3',4'} = J_{4',5'}$ 10.4 Hz, *H*-4′), 3.90−3.70 (5H, m, *H*-5, *H*-6a, *H*-5′, *H*-6′a, *H*-5″), 3.55−3.40 (3H, m, *H*-6b, *H*-6′b, *H*-6″a), 3.34 (1H, dd, $J_{5'',6''b}$ 4.7 Hz, $J_{6''a,6''b}$ 13.5 Hz, *H*-6″b), 2.10, 2.03, 2.02 (21H, 3s, 7 × C*H*$_3$CO); ^{13}C NMR (75 MHz, $CDCl_3$): δ = 170.7, 170.2, 170.1, 170.0, 169.6 (*C*O), 95.4, 95.3 (*C*-1′, *C*-1″), 86.4 (*C*-1), 71.9, 71.8, 71.5, 71.4, 70.8, 70.7, 70.5, 70.2, 69.6, 69.4, 69.3 (*C*-2 to *C*-5, *C*-2′ to *C*-5′, *C*-2″ to *C*-5″), 51.2, 51.0 (*C*-6, *C*-6′, *C*-6″), 21.1, 20.8, 20.7, 20.6 (*C*H$_3$CO); HRMS (ES+): Found 921.2601 $C_{32}H_{42}N_{12}O_{19}Na$ requires 921.2587 [M + Na^+].

2,3,4-Tri-*O*-acetyl-6-azido-6-deoxy-α-D-glucopyranosyl-(1 → 4)-2,3-di-*O*-acetyl-6-azido-6-deoxy-α-D-glucopyranosyl-(1 → 4)-2,3-di-*O*-acetyl-6-azido-6-deoxy-β-D-glucopyranosyl Azide (7). [α]$^{20}_D$ +108 (*c* 0.2, CH_2Cl_2); ^{1}H NMR (300 MHz, $CDCl_3$) δ = 5.39−5.25 (5H, m, *H*-1′, *H*-1″, *H*-3, *H*-3′, *H*-3″), 4.97 (1H, t, $J_{3'',4''} = J_{4'',5''}$ 9.0 Hz, *H*-4″), 4.81−4.63 (3H, m, *H*-2, *H*-2′, *H*-2″), 4.65 (1H, d, $J_{1,2}$ 8.8 Hz, *H*-1), 4.13 (1H, t, $J_{3,4} = J_{4,5}$ 9.3 Hz, *H*-4), 4.00 (1H, t, $J_{3',4'} = J_{4',5'}$ 9.4 Hz, *H*-4′), 3.90−3.70 (5H, m, *H*-5, *H*-6a, *H*-5′, *H*-6′a, *H*-5″), 3.55−3.40 (3H, m, *H*-6b, *H*-6′b *H*-6″a,), 3.32 (1H, dd, $J_{5'',6''b}$ 4.7 Hz, $J_{6''a,6''b}$ 13.5 Hz, *H*-6″b), 2.03, 2.02, 2.01,

1.99, 1.98 (21H, 5s, 7 × CH_3CO); ^{13}C NMR (75 MHz, $CDCl_3$): δ = 170.5, 170.2, 169.9, 169.5 (*C*O), 95.4, 95.2 (*C*-1′, *C*-1″), 87.5 (*C*-1), 76.1, 74.9, 71.6, 71.4, 70.6, 70.5, 70.1, 69.5, 69.2 (*C*-2 to *C*-5, *C*-2′ to *C*-5′, *C*-2″ to *C*-5″), 51.0, 50.9 (*C*-6, *C*-6′, *C*-6″), 21.0, 20.7, 20.6 (*C*H_3CO); HRMS (ES+): Found 921.2590 $C_{32}H_{42}N_{12}O_{19}$Na requires 921.2587 [M + Na^+].

1-[2,3,4,6-Tetra-*O*-acetyl-β-D-glucopyranos-1-yl]-4-[2,3,4,6-tetra-*O*-acetyl-α-D-mannopyranosyloxyethyl]-[1,2,3]-triazol (9). $[\alpha]^{20}_D$ +12 (*c* 0.1, CH_2Cl_2); ^{1}H NMR (300 MHz, $CDCl_3$) δ = 7.76 (1H, s, C*H*N), 5.80 (1H, d, $J_{1,2}$ 8.7 Hz, *H*-1), 5.45−5.25 (6H, m, *H*-2, *H*-3, *H*-4, *H*-2M, *H*-3M, *H*-4M), 4.79 (1H, s, *H*-1M), 4.23−3.95 (7H, m, *H*-5, *H*-6a, *H*-6b, *H*-5M, *H*-6aM, *H*-6bM, OC*H*aCH_2), 3.64−3.60 (1H, m, OC*H*bCH_2), 2.99 (2H, m, OCH_2CH_2), 2.09, 2.04, 1.98, 1.97, 1.95 (24H, 5s, 8 × CH_3CO); ^{13}C NMR (75 MHz, $CDCl_3$): δ = 170.7, 170.5, 170.3, 170.0, 169.7, 169.4, 168.7, (*C*O), 145.1 (N*C*═CH), 121.0 (NC═*C*H), 97.9 (*C*-1M), 85.8 (*C*-1), 75.0, 72.6, 70.6, 69.5, 69.2, 69.0, 67.9, 66.0 (*C*-2 to *C*-5, *C*-2M to *C*-5M), 67.2 (OCH_2CH_2), 62.5, 61.9 (*C*-6, *C*-6M), 26.3 (OCH_2CH_2), 20.9, 20.8, 20.7, 20.6, 20.1 (*C*H_3CO); HRMS (ES+): Found 796.2395 $C_{32}H_{43}N_3O_{19}$Na requires 796.2388 [M + Na^+].

1-[β-D-Glucopyranos-1-yl]-4-[α-D-mannopyranosyloxyethyl]-[1,2,3]-triazol (10). $[\alpha]^{20}_D$ +29 (*c* 0.4, H_2O); ^{1}H NMR (300 MHz, D_2O) δ = 8.04 (1H, s, C*H*N), 5.66 (1H, d, $J_{1,2}$ 8.7 Hz, H-1), 5.45−5.25 (6H, m, *H*-2, *H*-3, *H*-4, *H*-2M, *H*-3M, *H*-4M), 4.81 (1H, s, *H*-1M), 4.20−3.90 (13H, m, *H*-2 to *H*-5, *H*-6a, *H*-6b, *H*-2M to *H*-5M, *H*-6aM, *H*-6bM, OC*H*aCH_2), 3.65−3.60 (1H, m, OC*H*-bCH_2), 3.02 (2H, m, OCH_2CH_2); ^{13}C NMR (75 MHz, D_2O): δ = 145.9 (N*C*═CH), 123.5 (NC═*C*H), 97.7 (*C*-1M), 87.7 (*C*-1), 79.2, 76.3, 73.1, 72.7, 70.8, 70.4, 69.3, 66.9 (*C*-2 to *C*-5, *C*-2M to *C*-5M), 66.5 (OCH_2CH_2), 61.1, 60.8 (*C*-6, *C*-6M), 25.5 (OCH_2CH_2); HRMS (ES+): Found 460.1536 $C_{16}H_{27}N_3O_{11}$Na requires 460.1543 [M + Na^+].

2,3,4-Tri-*O*-acetyl-6-deoxy-6-[4-(2,3,4,6-tetra-*O*-acetyl-α-D-mannopyranosyloxyethyl)triazol-1-yl]-α-D-glucopyranosyl-(1 → 4)-1,2,3-tri-*O*-acetyl-6-deoxy-6-[4-(2,3,4,6-tetra-*O*-acetyl-α-D-mannopyranosyloxyethyl)triazol-1-yl]-D-glucopyranose (11). ^{1}H NMR (300 MHz, $CDCl_3$) δ = 7.57, 7.53 (4H, 2s, 2 × C*H*N$\alpha\beta$), 6.18 (1H, d, $J_{1,2}$ 3.7 Hz, *H*-1α), 5.67 (1H, d, $J_{1,2}$ 8.1 Hz, *H*-1*β*), 5.47−5.18 (18H, m, *H*-3, *H*-1′, *H*-3, *H*-3′, 2 × *H*-2M, 2 × *H*-3M, 2 × *H*-4M$\alpha\beta$), 4.81−4.45 (18H, m, *H*-2, *H*-6a, *H*-6b, *H*-2′, *H*-4′, *H*-6′a, *H*-6′b, 2 × H-1M$\alpha\beta$), 4.30−3.80 (20H, m, *H*-4, *H*-5, 2 × *H*-5M, 2 × *H*-6aM, 2 × *H*-6bM, 2 × OC*H*aC$H_2\alpha\beta$), 3.75−3.62 (6H, m, H-5′, 2 × OC*H*bC$H_2\alpha\beta$), 3.16−2.85 (8H, m, 2 × OCH_2C$H_2\alpha\beta$), 2.11, 2.07, 2.06, 2.04, 2.02, 2.01, 1.98, 1.97, 1.96 (84H, 9s, 14 × CH_3CO$\alpha\beta$); ^{13}C NMR (75 MHz, $CDCl_3$): δ = 170.8, 170.5, 170.1, 170.0, 169.9, 169.8, 169.6, 169.0, 168.8, 162.6, (*C*O), 144.4 (N*C*═CH), 124.5, 124.0 (NC═*C*H), 97.9, 97.7, 97.5 (*C*-1M), 95.7, 95.6 (*C*-1′$\alpha\beta$), 91.2 (*C*-1α), 88.6 (*C*-1*β*), 71.9, 72.0, 70.2, 69.9, 69.5, 69.4, 69.3, 69.2, 69.1, 68.7, 66.4 (*C*-2 to *C*-5, *C*-2′ to *C*-5′, *C*-2M to *C*-5M), 67.4, 67.2, 67.0 (OCH_2CH_2), 62.4 (*C*-6M), 50.0, 49.9, 49.7 (*C*-6, *C*-6′), 26.3 (OCH_2CH_2), 21.0, 20.8, 20.7, 20.5 (*C*H_3CO); HRMS (ES+): Found 1467.4607 $C_{60}H_{80}N_6O_{35}$Na requires 1467.4562 [M + Na^+].

6-Deoxy-6-[4-(α-D-mannopyranosyloxyethyl)triazol-1-yl]-α-D-glucopyranosyl-(1 → 4)-6-deoxy-6-[4-(α-D-mannopyranosyloxyethyl)triazol-1-yl]-D-glucopyranose (12). ^{1}H NMR (300 MHz, D_2O) δ = 7.78, 7.63, 7.60 (4H, 3s, 2 × C*H*N$\alpha\beta$), 5.23 (2H, d, $J_{1',2'}$ 3.3 Hz, *H*-1′$\alpha\beta$), 4.97 (1H, d, $J_{1,2}$ 3.7 Hz, *H*-1α), 4.79−4.25 (6H, m, *H*-6a, 2 × *H*-1M$\alpha\beta$), 4.39 (1H, d, $J_{1,2}$ 8.2 Hz, *H*-1*β*), 4.00−3.18 (48H, m, *H*-2 to *H*-5, *H*-6b, *H*-2′ to *H*-5′, *H*-6′a, *H*-6′b, 2 × *H*-2M to *H*-5M, 2 × *H*-6aM, 2 × *H*-6bM$\alpha\beta$), 3.15−3.00 (8H, m, 2 × OCH_2C$H_2\alpha\beta$), 2.75−2.50 (8H, m, 2 × OCH_2C$H_2\alpha\beta$); ^{13}C NMR (75 MHz, D_2O): δ = 145.5, 145.3 (N*C*═CH), 125.4, 125.1, 124.9 (NC═*C*H), 101.4 (*C*-1′), 100.1, 99.9 (*C*-1M), 96.0 (*C*-1*β*), 92.1 (*C*-1α), 75.9, 73.7, 73.2, 72.8, 72.5, 72.4, 72.0, 71.9, 71.4, 71.1, 70.9, 70.4, 68.1 (*C*-2 to *C*-5, *C*-2′ to *C*-5′, *C*-2M to *C*-5M), 66.9, 66.6, 66.4 (OCH_2CH_2), 61.2 (*C*-6M), 51.7, 50.5 (*C*-6, *C*-6′), 25.5, 25.2 (OCH_2CH_2). HRMS (ES+): Found 879.3080 $C_{32}H_{52}N_6O_{21}$Na requires 879.3083 [M + Na^+].

2,3,4-Tri-*O*-acetyl-6-deoxy-6-[4-(2,3,4,6-tetra-*O*-acetyl-α-D-mannopyranosyloxyethyl)triazol-1-yl]-α-D-glucopyranosyl-(1 → 4)-2,3-di-*O*-acetyl-6-deoxy-6-[4-(2,3,4,6-tetra-*O*-acetyl-α-D-mannopyranosyloxyethyl)triazol-1-yl]-α-D-glucopyranosyl-(1 → 4)-1,2,3-tri-*O*-acetyl-6-deoxy-6-[4-(2,3,4,6-tetra-*O*-acetyl-α-D-mannopyranosyloxyethyl)triazol-1-yl]-D-glucopyranose (13). ^{1}H NMR (300 MHz, $CDCl_3$) δ = 7.68, 7.66, 7.56, 7.54 (6H, 4s, 3 × C*H*N$\alpha\beta$), 6.22 (1H, d, $J_{1,2}$ 3.5 Hz, *H*-1α), 5.70 (1H, d, $J_{1,2}$ 8.0 Hz, *H*-1*β*), 5.50−5.15 (28H, m, *H*-3, *H*-1′, *H*-3′, *H*-1″, *H*-3″, 3 × *H*-2M, 3 × *H*-3M, 3 × *H*-4M$\alpha\beta$), 4.84−4.50 (28H, m, *H*-2, *H*-6a, *H*-6b, *H*-2′, *H*-4′, *H*-6′a, *H*-6′b, *H*-2″, *H*-4″, *H*-6″a, *H*-6″b, 3 × *H*-1M$\alpha\beta$), 4.45−4.20 (8H, m, *H*-5, 3 × *H*-6aM$\alpha\beta$), 4.10−3.82 (22H, m, *H*-4, *H*-5′, 3 × *H*-5M$\alpha\beta$, 3 × *H*-6bM$\alpha\beta$, 3 × OC*H*aC$H_2\alpha\beta$), 3.80−3.65 (8H, *H*-5″, 3 × OC*H*bC$H_2\alpha\beta$), 3.17−2.87 (12H, m, 3 × OCH_2C$H_2\alpha\beta$), 2.11, 2.07, 2.06, 2.01, 2.00, 1.97, 1.95, 1.93 (120H, 8s, 20 × CH_3CO$\alpha\beta$); ^{13}C NMR (75 MHz, $CDCl_3$): δ = 170.7, 170.5, 170.4, 170.1, 170.0, 169.8, 169.6, 169.4, 169.1 (*C*O), 144.4, 144.3, 144.0, 143.9 (N*C*═CH), 124.9, 124.7, 124.0 (NC═*C*H), 97.8, 97.6 (*C*-1M), 95.9, 95.3 (*C*-1′), 91.3 (*C*-1α), 88.7 (*C*-1*β*), 74.5, 74.1, 73.4, 73.3, 72.3, 72.2, 71.8, 70.5, 70.3, 69.8, 69.5, 69.2, 68.6, 66.1 (*C*-2 to *C*-5, *C*-2′ to *C*-5′, *C*-2″ to *C*-5″, *C*-2M to *C*-5M), 67.3, 67.1 (OCH_2CH_2), 62.4 (*C*-6M), 50.0, 49.7, 49.2 (*C*-6, *C*-6′, *C*-6″), 26.1 (OCH_2CH_2), 21.1, 21.0, 20.8, 20.7, 20.5 (*C*H_3CO); HRMS (ES+): Found 2138.6636 $C_{88}H_{117}N_9O_{51}$Na requires 2138.6736 [M + Na^+].

6-Deoxy-6-(4-(mannopyranosyloxyethyl)triazol-1-yl))-α-D-glucopyranosyl-(1 → 4)-6-deoxy-6-(4-(mannopyranosyloxyethyl)triazol-1-yl))-α-D-glucopyranosyl-(1 → 4)-6-deoxy-6-(4-(mannopyranosyloxyethyl)triazol-1-yl))-D-glucopyranose (14). ^{1}H NMR (300 MHz, D_2O) δ = 7.77, 7.65, 7.61, 7.57 (6H, 4s, 3 × C*H*N$\alpha\beta$), 5.27 (2H, d, $J_{1'',2''}$ 3.8 Hz, *H*-1″$\alpha\beta$) (assignments may be interchanged), 5.16 (2H, d, $J_{1',2'}$ 3.8 Hz, H-1′$\alpha\beta$)″$\alpha\beta$) (assignments may be interchanged), 4.95 (1H, d, $J_{1,2}$ 3.6 Hz, H-1α), 4.82−4.70 (8H, m, *H*-6a, 3 × *H*-1M$\alpha\beta$), 4.45−4.36 (2H, m, *H*-6b$\alpha\beta$), 4.38 (1H, d, $J_{1,2}$ 7.8 Hz, H-1*β*), 4.10−3.00 (68H, m, *H*-2 to *H*-5, *H*-2′ to *H*-5′, *H*-6′a, *H*-6′b, *H*-2″ to *H*-5″, *H*-6″a, *H*-6″b, 3 × *H*-2M to *H*-5M, 3 × *H*-6aM, 3 × *H*-6bM$\alpha\beta$), 3.00−2.95 (12H, m, 3 × OCH_2CH_2), 2.70−2.40 (m, 3 × OCH_2CH_2). ^{13}C NMR (75 MHz, D_2O): δ = 145.5, 145.2 (N*C*═CH), 125.3, 125.1, 124.9 (NC═*C*H), 101.5 (*C*-1′)″$\alpha\beta$) (assignments may be interchanged), 101.0 (*C*-1′)″$\alpha\beta$) (assignments may be interchanged), 100.1 (*C*-1M), 96.0 (*C*-1*β*), 92.0 (*C*-1α), 81.7, 81.4, 81.3, 75.9, 73.7, 73.1, 72.8, 72.6, 71.9, 71.3, 70.9, 70.4, 67.1, 66.9 (*C*-2 to *C*-5, *C*-2′ to *C*-5′, *C*-2″ to *C*-5″, *C*-2M to *C*-5M), 66.6, 66.4, 66.2 (OCH_2CH_2), 61.2 (*C*-6M), 51.7, 51.0, 50.3 (*C*-6, *C*-6′, *C*-6″), 25.5, 25.2 (OCH_2CH_2); HRMS (ES+): Found 1298.4572 $C_{48}H_{77}N_9O_{31}$Na requires 1298.4623 [M + Na^+].

1-{2,3,4-Tri-*O*-acetyl-6-deoxy-6-[1-(2,3,4,6-tetra-*O*-acetyl-α-D-mannopyranosyloxyethyl)triazol-4-yl]-α-D-glucopyranosyl-(1 → 4)-2,3-di-*O*-acetyl-6-deoxy-6-[1-(2,3,4,6-tetra-*O*-acetyl-α-D-mannopyranosyloxyethyl)triazol-4-yl]-β-D-glucopyranos-1-yl}-4-[2,3,4,6-tetra-*O*-acetyl-α-D-mannopyranosyloxyethyl]-[1,2,3]-triazol (15). $[\alpha]^{20}_D$ +43 (*c* 0.1, CH_2Cl_2); ^{1}H NMR (300 MHz, $CDCl_3$) δ = 7.59, 7.54, 7.41 (3H, 3s, 3 × C*H*N), 5.83 (1H, d, $J_{1,2}$ 9.1 Hz, *H*-1), 5.50−5.10 (12H, m, *H*-3, *H*-1′, *H*-3′, 3 × *H*-2M, 3 × *H*-3M, 3 × *H*-4M), 4.82−4.50 (10H, m, *H*-2, *H*-6a, *H*-6b, *H*-2′, *H*-4′, *H*-6′a, *H*-6′b, 3 × *H*-1M), 4.25−3.50 (18H, m, *H*-4, *H*-5, *H*-5′, 3 × *H*-5M, 3 × *H*-6aM, 3 × *H*-6bM, 3 × OCH_2CH_2), 3.12−2.80 (6H, m, 3 × OCH_2CH_2), 2.09, 2.07, 2.05, 2.04, 2.03, 2.02, 2.00, 1.99, 1.97, 1.95 (51H, 10s 17 × CH_3CO); ^{13}C NMR (75 MHz, $CDCl_3$): δ = 170.7, 170.4, 170.2, 170.1, 169.9, 169.7, 169.6, 168.9 (*C*O), 144.9, 144.3 (N*C*═CH), 123.9, 123.8, 121.2 (NC═*C*H), 97.9, 97.8, 97.5 (*C*-1M), 96.0 (*C*-1′), 85.0 (*C*-1), 75.4, 74.5, 73.5, 70.9, 70.0, 69.5, 69.3, 69.1, 66.0 (*C*-2 to *C*-5, *C*-2′ to *C*-5′, *C*-2M to *C*-5M), 67.2, 67.1, 66.9 (OCH_2CH_2), 62.5 (*C*-6M), 50.3, 50.0 (*C*-6, *C*-6′), 26.1 (OCH_2CH_2), 20.9, 20.8 (*C*H_3CO); HRMS (ES+): Found 1850.5839 $C_{76}H_{101}N_9O_{43}$Na requires 1850.5891 [M + Na^+].

1-{6-Deoxy-6-[1-(α-D-mannopyranosyloxyethyl)triazol-4-yl]-α-D-glucopyranosyl-(1 → 4)-6-deoxy-6-[1-(ϵπ-mannopyranosy-

loxyethyl)triazol-4-yl]-β-D-glucopyranos-1-yl}-4-[α-D-mannopyranosyloxyethyl]-[1,2,3]-triazol (16). $[\alpha]^{20}_D$ +57 (*c* 0.1, H_2O); ^1H NMR (300 MHz, D_2O) δ = 7.89, 7.83, 7.55 (3H, 3s, 3 × C*H*N), 5.55 (1H, d, $J_{1,2}$ 8.6 Hz, *H*-1), 5.34 (1H, d, $J_{1',2'}$ 3.7 Hz, *H*-1′), 4.75−4.65 (4H, m, *H*-6a, 3 × *H*-1M), 4.55 (1H, dd, $J_{5,6b}$ 9.3 Hz, $J_{6a,6b}$ 14.7 Hz, *H*-6b), 4.30−3.25 (34H, m, *H*-2 to *H*-5, *H*-2′ to *H*-5′, *H*-6′a, *H*-6′b, 3 × *H*-2M to *H*-5M, 3 × *H*-6aM, 3 × *H*-6bM, 3 × OC*H*$_2$CH$_2$), 3.12−2.85 (4H, m, 2 × OCH$_2$C*H*$_2$), 2.72−2.50 (2H, m, OCH$_2$C*H*$_2$); ^{13}C NMR (75 MHz, D_2O): δ = 145.8, 145.4, 145.2 (N*C*═CH), 125.5, 125.0, 123.2 (NC═*C*H), 101.5 (*C*-1′), 99.9 (*C*-1M), 87.1 (*C*-1), 80.4, 76.1, 75.0, 73.1, 72.7, 72.4, 71.9, 71.3, 70.9, 70.8, 70.3, 66.9 (*C*-2 to *C*-5, *C*-2′ to *C*-5′, *C*-2M to *C*-5M), 66.4, 66.3 (O*C*H$_2$CH$_2$), 61.1 (*C*-6M), 51.7, 50.2 (*C*-6, *C*-6′), 25.4, 25.2 (OCH$_2$*C*H$_2$); HRMS (ES+): Found 1136.4042 $C_{42}H_{67}N_9O_{26}Na$ requires 1136.4095 [M + Na^+].

1-{2,3,4-Tri-*O*-acetyl-6-deoxy-6-[1-(2,3,4,6-tetra-*O*-acetyl-α-D-mannopyranosyloxyethyl)triazol-4-yl]-α-D-glucopyranosyl-(1 → 4)-2,3-di-*O*-acetyl-6-deoxy-6-[1-(2,3,4,6-tetra-*O*-acetyl-α-D-mannopyranosyloxyethyl)triazol-4-yl]-α-D-glucopyranos-1-yl}-4-[2,3,4,6-tetra-*O*-acetyl-α-D-mannopyranosyloxyethyl]-[1,2,3]-triazol (17). $[\alpha]^{20}_D$ +58 (*c* 0.4, CH_2Cl_2); ^1H NMR (300 MHz, $CDCl_3$) δ = 7.59, 7.57, 7.55 (3H, 3s, 3 × C*H*N), 6.30 (1H, d, $J_{1,2}$ 5.6 Hz, *H*-1), 6.00 (1H, t, $J_{2,3}$ = $J_{3,4}$ 7.4 Hz, *H*-3), 5.48 (1H, d, $J_{1',2'}$ 3.8 Hz, *H*-1′), 5.45−5.15 (11H, m, *H*-2, *H*-3′, 3 × *H*-2M, 3 × *H*-3M, 3 × *H*-4M), 4.80−4.62 (9H, m, *H*-6a, *H*-6b, *H*-2′, *H*-4′, *H*-6′a, *H*-6′b, 3 × *H*-1M), 4.50−3.60 (18H, m, *H*-4, *H*-5, *H*-5′, 3 × *H*-5M, 3 × *H*-6aM, 3 × *H*-6bM, 3 × OC*H*$_2$CH$_2$), 3.12−2.82 (6H, m, 3 × OCH$_2$C*H*$_2$), 2.09, 2.08, 2.06, 2.05, 2.02, 1.98, 1.95 (51H, 7s, 17 × C*H*$_3$CO); ^{13}C NMR (75 MHz, $CDCl_3$): δ = 170.7, 170.5, 170.3, 170.1, 170.0, 169.8, 169.7, 169.5 (*C*O), 144.5, 144.1, 143.8 (N*C*═CH), 124.4, 123.9, 123.6 (NC═*C*H), 97.6, 97.5 (*C*-1M), 95.5 (*C*-1′), 81.1 (*C*-1), 72.8, 72.0, 71.4, 69.5, 69.4, 69.1, 68.8, 68.6, 66.0, 65.9, 65.8 (*C*-2 to *C*-5, *C*-2′ to *C*-5′, *C*-2M to *C*-5M), 67.0, 66.8 (O*C*H$_2$CH$_2$), 62.4 (*C*-6M), 50.1, 49.5 (*C*-6, *C*-6′), 26.0 (OCH$_2$*C*H$_2$), 20.9, 20.8, 20.7, 20.3 (*C*H$_3$CO); HRMS (ES+): Found 1850.5936 $C_{76}H_{101}N_9O_{43}Na$ requires 1850.5891 [M + Na^+].

1-{6-Deoxy-6-[1-(α-D-mannopyranosyloxyethyl)triazol-4-yl]-α-D-glucopyranosyl-(1 → 4)-6-deoxy-6-[1-(α-D-mannopyranosyloxyethyl)triazol-4-yl]-α-D-glucopyranos-1-yl}-4-[α-D-mannopyranosyloxyethyl]-[1,2,3]-triazol (18). $[\alpha]^{20}_D$ +47 (*c* 0.1, H_2O); ^1H NMR (300 MHz, D_2O) δ = 7.78, 7.71, 7.54 (3H, 3s, 3 × C*H*N), 6.08 (1H, d, $J_{1,2}$ 5.9 Hz, *H*-1), 5.30 (1H, d, $J_{1',2'}$ 3.7 Hz, *H*-1′), 4.92−4.65 (4H, m, *H*-6a, 3 × *H*-1M), 4.50−4.32 (2H, m, *H*-3, *H*-6b), 4.10−3.20 (33H, m, *H*-2, *H*-4, *H*-5, *H*-2′ to *H*-5′, *H*-6′a, *H*-6′b, 3 × *H*-2M to *H*-5M, 3 × *H*-6′a, 3 × *H*-6′b, 3 × OC*H*$_2$-CH$_2$), 3.00−2.80 (4H, m, 2 × OCH$_2$C*H*$_2$), 2.62−2.50 (2H, m, OCH$_2$C*H*$_2$); ^{13}C NMR (75 MHz, D_2O): δ = 147.8, 147.6 (N*C*═CH), 128.1, 128.0, 127.5 (NC═*C*H), 103.8 (*C*-1′), 102.6, 102.5 (*C*-1M), 87.0 (*C*-1), 83.1, 76.1, 75.7, 75.6, 75.3, 74.9, 74.5, 74.2, 73.9, 73.5, 73.4, 72.8, 72.4 (*C*-2 to *C*-5, *C*-2′ to *C*-5′, *C*-2M to *C*-5M), 69.5, 69.4 (O*C*H$_2$CH$_2$), 69.1, 68.9 (*C*-6M), 54.2, 52.6 (*C*-6, *C*-6′), 28.0, 27.8, 27.7 (OCH$_2$*C*H$_2$); HRMS (ES+): Found 1136.4055 $C_{42}H_{67}N_9O_{26}Na$ requires 1136.4095 [M + Na^+].

1-{2,3,4-Tri-*O*-acetyl-6-[1-(2,3,4,6-tetra-*O*-acetyl-α-D-mannopyranosyloxyethyl)triazol-4-yl]-6-deoxy-α-D-glucopyranosyl-(1 → 4)-2,3-di-*O*-acetyl-6-[1-(2,3,4,6-tetra-*O*-acetyl-α-D-mannopyranosyloxyethyl)triazol-4-yl]-6-deoxy-α-D-glucopyranosyl-(1 → 4)-2,3-di-*O*-acetyl-6-deoxy-6-[1-(2,3,4,6-tetra-*O*-acetyl-α-D-mannopyranosyloxyethyl)triazol-4-yl]-β-D-glucopyranos-1-yl}-[1,2,3]-4-[2,3,4,6-tetra-*O*-acetyl-α-D-mannopyranosyloxyethyl-]triazol (19). $[\alpha]^{20}_D$ +46 (*c* 0.2, CH_2Cl_2); ^1H NMR (300 MHz, $CDCl_3$) δ = 7.63, 7.59, 7.52, 7.42, (4H, 4s, 4 × C*H*N), 5.85 (1H, d, $J_{1,2}$ 9.1 Hz, *H*-1), 5.50−5.05 (17H, m, *H*-3, *H*-1′, *H*-3′, *H*-1″, *H*-3″, 4 × *H*-2M, 4 × *H*-3M, 4 × *H*-4M), 4.83−4.35 (14H, m, *H*-2, *H*-6a, *H*-6b, *H*-2′, *H*-6′a, *H*-6′b, *H*-2″, *H*-4″, *H*-6″a, *H*-6″b, 4 × *H*-1M), 4.22−3.50 (25H, m, *H*-4, *H*-5, *H*-4′, *H*-5′, *H*-5″, 4 × *H*-5M, 4 × *H*-6aM, 4 × *H*6bM, 4 × OC*H*$_2$CH$_2$), 3.10−2.80 (8H, m, 4 × OCH$_2$C*H*$_2$), 2.08, 2.05, 2.03, 2.01, 1.99, 1.98, 1.96, 1.94, 1.92, 1.91 (69H, 10s, 23 × C*H*$_3$CO); ^{13}C NMR (75 MHz, $CDCl_3$): δ = 170.7, 170.3, 170.2, 170.1, 169.8, 169.7, 169.4 (*C*O), 144.9, 144.2, 144.0 (N*C*═CH), 124.7, 123.9, 121.3 (NC═*C*H), 97.8, 97.7, 97.6, 97.5 (*C*-1M), 95.8, 95.2 (*C*-1′, *C*-1″), 84.9 (*C*-1), 74.0, 70.4, 69.8, 69.5, 69.4, 69.3, 69.1, 68.8, 68.7, 68.6, 66.0, 65.9 (*C*-2 to *C*-5, *C*-2′ to *C*-5′, *C*-2″ to *C*-5″, *C*-2M to *C*-5M), 67.2, 67.0 (O*C*H$_2$-CH$_2$), 62.3 (*C*-6M), 49.9, 49.4 (*C*-6, *C*-6′, *C*-6″), 26.0 (OCH$_2$*C*H$_2$), 20.9, 20.7, 20.1 (*C*H$_3$CO); HRMS (ES+): Found 2521.8158 $C_{104}H_{138}N_{12}O_{59}Na$ requires 2521.8065 [M + Na^+].

1-{6-Deoxy-6-[1-(α-D-mannopyranosyloxyethyl)triazol-4-yl]-α-D-glucopyranosyl-(1 → 4)-6-deoxy-6-[1-(α-D-mannopyranosyloxyethyl)triazol-4-yl]-α-D-glucopyranosyl-(1 → 4)-6-deoxy-6-[1-(α-D-mannpyranosyloxyethyl)triazol-4-yl]-β-D-glucopyranos-1-yl}-4-[α-D-mannopyranosyloxyethyl]-[1,2,3]-triazol (20). $[\alpha]^{20}_D$ +57 (*c* 0.1, H_2O); ^1H NMR (300 MHz, D_2O) δ = 7.86, 7.81, 7.69, 7.52 (4H, 4s, 4 × C*H*N), 5.52 (1H, d, $J_{1,2}$ 8.5 Hz, *H*-1), 5.32 (1H, d, $J_{1'',2''}$ 3.7 Hz, *H*-1″)″αβ) (assignments may be interchanged), 5.26 (1H, d, $J_{1',2'}$ 3.9 Hz, *H*-1′)″αβ) (assignments may be interchanged), 4.90−4.70 (5H, m, *H*-6a, 4 × *H*-1M), 4.60−4.40 (1H, dd, $J_{5,6b}$ 9.3 Hz, $J_{6a,6b}$ 14.7 Hz, *H*-6b), 4.20−3.20 (48H, m, *H*-2 to *H*-5, *H*-2′ to *H*-5′, *H*-6′a, *H*-6′b, *H*-2″ to *H*-5″, *H*-6″a, *H*-6″b, 4 × *H*-2M to *H*-5M, 4 × *H*-6aM, 4 × *H*-6bM, 4 × OC*H*$_2$CH$_2$), 3.10−2.80 (4H, m, 2 × OCH$_2$C*H*$_2$), 2.72−2.45 (4H, m, 2 × OCH$_2$C*H*$_2$); ^{13}C NMR (75 MHz, D_2O): δ = 145.8, 145.4, 145.2 (N*C*═CH), 125.3, 125.0, 123.2 (NC═*C*H), 101.5, 101.2 (*C*-1′, *C*-1″), 100.0, 99.9 (*C*-1M), 87.0 (*C*-1), 81.4, 80.5, 75.9, 74.8, 73.2, 72.7, 72.5, 71.8, 70.9, 70.8, 70.7, 70.3, 67.0, 66.9 (*C*-2 to *C*-5, *C*-2′ to *C*-5′, *C*-2″ to *C*-5″, *C*-2M to *C*-5M), 66.3, 66.1 (O*C*H$_2$-CH$_2$), 61.1 (*C*-6M), 51.6, 50.9, 49.9 (*C*-6, *C*-6′, *C*-6″), 25.4, 25.1 (OCH$_2$*C*H$_2$); HRMS (ES+): Found 1555.5693 $C_{58}H_{92}N_{12}O_{36}Na$ requires 1555.5635 [M + Na^+].

1-{2,3,4-Tri-*O*-acetyl-6-deoxy-6-[1-(2,3,4,6-tetra-*O*-acetyl-α-D-mannopyranosyloxyethyl)triazol-4-yl]-α-D-glucopyranosyl-(1 → 4)-2,3-di-*O*-acetyl-6-deoxy-6-[1-(2,3,4,6-tetra-*O*-acetyl-α-D-mannopyranosyloxyethyl)triazol-4-yl]-α-D-glucopyranosyl-(1 → 4)-2,3-di-*O*-acetyl-6-deoxy-6-[1-(2,3,4,6-tetra-*O*-acetyl-α-D-mannopyranosyloxyethyl)triazol-4-yl]-α-D-glucopyranos-1-yl}-4-[2,3,4,6-tetra-*O*-acetyl-β-D-mannopyranosyloxyethyl]-[1,2,3]-triazol (21). $[\alpha]^{20}_D$ +64 (*c* 0.1, CH_2Cl_2); ^1H NMR (300 MHz, $CDCl_3$) δ = 7.72, 7.66, 7.59 (4H, 3s, 4 × C*H*N), 6.30 (1H, d, $J_{1,2}$ 5.6 Hz, *H*-1), 6.03 (1H, t, $J_{2,3}$ = $J_{3,4}$ 7.4 Hz, *H*-3), 5.47 (1H, d, $J_{1'',2''}$ 3.8 Hz, *H*-1″), 5.46−5.05 (17H, m, *H*-2, *H*-1′, *H*-2′, *H*-3′, *H*-3″, 4 × *H*-2M, 4 × *H*-3M, 4 × *H*-4M), 5.00−4.35 (14H, m, *H*-4, *H*-6a, *H*-6b, *H*-4′, *H*-6′a, *H*-6′b, *H*-2″, *H*-4″, *H*-6″a, *H*-6″b, 4 × *H*-1M), 4.32−3.65 (23H, m, *H*-5, *H*-5′, *H*-5″, 4 × *H*-5M, 4 × *H*-6aM, 4 × *H*-6bM, 4 × OC*H*$_2$CH$_2$), 3.20−2.85 (8H, m, 4 × OCH$_2$C*H*$_2$), 2.12, 2.10, 2.09, 2.07, 2.05, 2.00, 1.99, 1.98, 1.95, 1.93 (69H, 10s, 23 × C*H*$_3$CO); ^{13}C NMR (75 MHz, $CDCl_3$): δ = 170.7, 170.4, 170.2, 169.8, 169.7, 169.6, 169.4 (*C*O), 144.5, 143.9 (N*C*═CH), 124.9, 124.6, 123.9, 123.7 (NC═*C*H), 97.6, 97.5 (*C*-1M), 95.6, 95.3 (*C*-1′, *C*-1″), 81.2 (*C*-1), 72.1, 70.0, 69.5, 68.8, 68.7, 68.6, 66.0, 65.9, 65.8 (*C*-2 to *C*-5, *C*-2′ to *C*-5′, *C*-2″ to *C*-5″, *C*-2M to *C*-5M), 67.2, 67.1, 66.9 (O*C*H$_2$CH$_2$), 62.4 (*C*-6M), 49.9, 49.6, 49.2 (*C*-6, *C*-6′, *C*-6″), 26.1 (OCH$_2$*C*H$_2$), 20.9, 20.8, 20.4 (*C*H$_3$CO); HRMS (ES+): Found 2521.8137 $C_{104}H_{138}N_{12}O_{59}Na$ requires 2521.8065 [M + Na^+].

1-{6-Deoxy-6-[1-(α-D-mannopyranosyloxyethyl)triazol-4-yl]-α-D-glucopyranosyl-(1 → 4)-6-[1-(α-D-mannopyranosyloxyethyl)triazol-4-yl]-6-deoxy-α-D-glucopyranosyl-(1 → 4)-6-(α-D-mannopyranosyloxyethyl)triazol-4-yl]-6-deoxy-β-D-glucopyranos-1-yl}-4-[α-D-mannopyranosyloxyethyl]-[1,2,3]-triazol (22). $[\alpha]^{20}_D$ +56 (*c* 0.1, H_2O); ^1H NMR (300 MHz, D_2O) δ = 7.79, 7.74, 7.67, 7.55 (4H, 4s, 4 × C*H*N), 6.08 (1H, d, $J_{1,2}$ 5.9 Hz, *H*-1), 5.31 (1H, d, $J_{1'',2''}$ 3.6 Hz, *H*-1″)″αβ) (assignments may be interchanged), 5.26 (1H, d, $J_{1',2'}$ 3.7 Hz, *H*-1′)″αβ) (assignments may be interchanged), 4.90−4.68 (5H, m, *H*-6a, 4 × *H*-1M), 4.50−4.35 (2H, m, *H*-3, *H*-6b), 4.22−3.20 (47H, m, *H*-2, *H*-4, *H*-5, *H*-2′ to *H*-5′, *H*-6′a, *H*-6′b, *H*-2″ to *H*-5″, *H*-6″a, *H*-6″b, 4 × *H*-2M to *H*-5M, 4 × *H*-6aM, 4 × *H*-6bM, 4 × OC*H*$_2$CH$_2$), 3.05−2.80 (4H, m, 2 × OCH$_2$C*H*$_2$), 2.60−2.45 (4H, m, 2 × OCH$_2$C*H*$_2$); ^{13}C NMR

(75 MHz, D_2O): δ = 145.3, 145.1, 145.0 (NC=CH), 125.5, 125.3, 125.0 (NC=CH), 101.5, 100.9 (*C*-1′, *C*-1″), 100.1, 99.9 (*C*-1M), 84.4 (*C*-1), 81.3, 80.6, 73.2, 73.0, 72.7, 72.5, 71.8, 71.5, 71.3, 70.9, 70.8, 70.3, 69.8, 67.0, 66.9 (*C*-2 to *C*-5, *C*-2′ to *C*-5′, *C*-2″ to *C*-5″, *C*-2M to *C*-5M), 66.5, 66.3, 66.1 (OCH_2CH_2), 61.2, 61.1 (*C*-6M), 51.6, 50.9, 49.8 (*C*-6, *C*-6′, *C*-6″), 25.4, 25.1 (OCH_2CH_2); HRMS (ES+): Found 1555.5637 $C_{58}H_{92}N_{12}O_{36}Na$ requires 1555.5635 [M + Na^+].

Atom Charge Value Derivation, Building, and Validation of a New FFTPDB. β-D-Glucose, α-D-glucose, methyl α-D-glucopyranoside, methyl α-D-mannopyranoside, and 1-*N*-methyl-4-(2-hydroxyethyl)-1,2,3-triazole were involved in the charge derivation procedure. The ω dihedral angle conformations *gg* and *gt* were chosen for the glucose and mannose derivatives,[39] while the two lowest minima for 1-*N*-methyl-4-(2-hydroxyethyl)-1,2,3-triazole found after geometry search were selected. The geometries of the glucose and mannose derivatives were optimized using dihedral angle constraints. The HO4′−O4′−C4′−H4′ dihedral angle of the monosaccharides was constrained to a value of 180°. A second constraint for the HO2′−O2′−C2′−H2′ dihedral angle of β-glucose and for the HO3′−O3′−C3′−H3′ dihedral angle of methyl α-mannopyranoside was used and set to values of 180 and 60°, respectively. Frequencies were calculated for all the molecules. Geometry optimization, frequency calculation, and MEP computation were carried out using the Gaussian 98 program in the gas phase,[45] while charge fitting was performed using the RESP program.[38a] The HF/6-31G** theory level was used in geometry optimization and frequency calculation.[43] The MEP computation was carried out using the HF/6-31G* theory level[43] and the CHELPG algorithm.[46] The molecular orientation of the optimized geometries was controlled using the rigid-body reorientation algorithm implemented in the R.E.D. program before MEP computation,[41] and four orientations (based on the C1′ C3′ C5′, C5′ C3′ C1′, C2′ C4′ O5′, and O5′ C4′ C2′ atom names for glucose and mannose derivatives and based on the OH C1 C2, C2 C1 OH, C2 C3 N4, and N4 C3 C2 atom names for the triazole derivative) were generated for each optimized geometry. Charge fitting was performed using a single RESP stage and a hyperbolic constraint value of 0.01.[37,38b] Inter-molecular charge constraints between the methyl group of methyl α-D-glucopyranoside, methyl α-D-mannopyranoside, and 1-*N*-methyl-4-(2-hydroxyethyl)-1,2,3-triazole, the anomeric 4- or 6-hydroxyl group of methyl α-D-glucopyranoside, β-D-glucose, and α-D-glucose, or the hydroxyl group of 1-*N*-methyl-4-(2-hydroxyethyl)-1,2,3-triazole were set to a target value of zero in the charge fitting procedure. Intra-molecular charge constraints between the methyl and the 4-hydroxyl groups of methyl α-D-glucopyranoside, and for each hydrogen bound to a sp^3 carbon, were also set to a value of zero. The charge derivation procedure was automatically carried out using a version IV β of the R.E.D. program.[41] The RESP atom charge values and the FFTPDB were submitted in R.E.DD.B. and are available as the "F-71" R.E.DD.B. project code. The FFTPDB is available as a suite of molecular fragments in the Tripos mol2 file format and is used to build AMBER OFF force field libraries. A LEaP script is available in the "F-71" R.E.DD.B. project for this purpose.[47]

To validate the glycocluster FFTPDB reported, a comparative study involving the glucose scaffold [disaccharide Glc-α-(1 → 4) α-Glc] was carried out using the molecular fragments and RESP charge values taken from the Glycam 2004 force field and the FFTPDB described in this work. However, in the absence of the hemiacetal hydroxyl fragment and the corresponding charge values in the Glycam 2004 force field version available in the AMBER 8 distribution, the charge values were derived anew for this missing fragment. Charge values were obtained following standard procedures implemented in the R.E.D. program as previously described.[41] This was carried out using methanol and an intra-molecular charge constraint for the methyl group set to the sum of charge values found in the 1GA and 4GA glucose fragments during the fit. Charge values of −0.6131 and 0.4141 were found for the oxygen and hydrogen atoms, respectively, and used to build a LEaP library for this additional fragment leading to the HO-4GA-1GA tri-unit-based disaccharides.

Molecular Dynamics Simulation. Three-dimensional structures and dynamics of the glucose scaffold [disaccharide Glc-α-(1 → 4) α-Glc] and glycoclusters **12**β, **12**α, **16**, and **18** were studied using the AMBER 8 program.[48] Each structure was solvated in a truncated octahedron box of TIP3P explicit water[49] and subjected to 10 ns constant pressure productive MD at 300 K after a 225 ps period of constant volume equilibration.[50] 3 ns constant pressure productive MD was also performed at 320 and 340 K for checking putative trapping of simulation in local minima. Geometry optimization and unrestrained MD simulations were carried out using force field parameters taken from the Glycam 2004 force field,[37] and the FFTPDB was reported. Missing force field parameters for the triazole and hemiacetal derivatives were obtained from the General AMBER force field.[51] A cutoff value of 9.0 Å and a time step value of 0.002 ps with the SHAKE algorithm for constraining bonds involving hydrogens were used during the simulations.[52] The 1−4 van der Waals and 1−4 electrostatics interactions were divided by a scaling factor value of 1.0 as suggested by the Glycam 2004 force field authors.[37] MD was carried out on a PC workstation with an Intel Core 2 Duo E6400 CPU under a Fedora Core 6 Linux distribution (http://fedoraproject.org/). Finally, the geometry of model compounds for each minimum observed during MD simulation was further characterized and optimized by ab initio in the gas phase using the B3LYP/6-311+G** theory level.[43] Molecular visualization, structure comparison, and structural properties of the PDB structures and MD snapshots were analyzed using the ptraj module of the AMBER 8, VMD,[53] and InsightII 2000 (Accelrys Inc., San Diego, CA) programs.

(45) Frisch, M. J.; Trucks, G. W.; Schlegel, H. B.; Scuseria, G. E.; Robb, M. A.; Cheeseman, J. R.; Zakrzewski, V. G.; Montgomery, J. A., Jr.; Stratmann, R. E.; Burant, J. C.; Dapprich, S.; Millam, J. M.; Daniels, A. D.; Kudin, K. N.; Strain, M. C.; Farkas, O.; Tomasi, J.; Barone, V.; Cossi, M.; Cammi, R.; Mennucci, B.; Pomelli, C.; Adamo, C.; Clifford, S.; Ochterski, J.; Petersson, G. A.; Ayala, P. Y.; Cui, Q.; Morokuma, K.; Malick, D. K.; Rabuck, A. D.; Raghavachari, K.; Foresman, J. B.; Cioslowski, J.; Ortiz, J. V.; Baboul, A. G.; Stefanov, B. B.; Liu, G.; Liashenko, A.; Piskorz, P.; Komaromi, I.; Gomperts, R.; Martin, R. L.; Fox, D. J.; Keith, T.; Al-Laham, M. A.; Peng, C. Y.; Nanayakkara, A.; Gonzalez, C.; Challacombe, M.; Gill, P. M. W.; Johnson, B.; Chen, W.; Wong, M. W.; Andres, J. L.; Gonzalez, C.; Head-Gordon, M.; Replogle, E. S.; Pople, J. A. *Gaussian 98*, revision A.11; Gaussian, Inc.: Pittsburgh, PA, 1998.

(46) Breneman, C. M.; Wiberg, K. B. *J. Comput. Chem.* **1990**, *11*, 361−373.

(47) Schafmeister, C. E. A. F.; Ross, W. S.; Romanovski, V. *LEaP*; University of California, San Francisco: San Francisco, 1995.

(48) (a) Pearlman, D. A.; Case, D. A.; Caldwell, J. W.; Ross, W. S.; Cheatham, T. E., III; DeBolt, S.; Ferguson, D.; Seibel, G.; Kollman, P. A. *Comput. Phys. Commun.* **1995**, *91*, 1−41. (b) Case, D. A.; Darden, T. A.; Cheatham, T. E., III; Simmerling, C. L.; Wang, J.; Duke, R. E.; Luo, R.; Merz, K. M.; Wang, B.; Pearlman, D. A.; Crowley, M.; Brozell, S.; Tsui, V.; Gohlke, H.; Mongan, J.; Hornak, V.; Cui, G.; Beroza, P.; Schafmeister, C.; Caldwell, J. W.; Ross, W. S.; Kollman, P. A. *AMBER 8*; University of California, San Francisco: San Francisco, 2004.

(49) Jorgensen, W. L.; Chandrasekhar, J.; Madura, J.; Klein, M. L. *J. Chem. Phys.* **1983**, *79*, 926−935.

(50) Dupradeau, F.-Y.; Case, D. A.; Yu, C.; Jimenez, R.; Romesberg, F. E. *J. Am. Chem. Soc.* **2005**, *127*, 15612−15617.

(51) Wang, J.; Wolf, R. M.; Caldwell, J. W.; Kollman, P. A.; Case, D. A. *J. Comput. Chem.* **2004**, *25*, 1157−1174.

(52) Ryckaert, J.-P.; Ciccotti, G.; Berendsen, H. J. C. *J. Comput. Phys.* **1977**, *23*, 327−341.

(53) Humphrey, W.; Dalke, A.; Schulten, K. *J. Mol. Graphics* **1996**, *14*, 33−38.

Acknowledgment. This work was carried out with financial support from the Centre National de la Recherche Scientifique and the Ministère Délégué à l'Enseignement Supérieur et à la Recherche.

Supporting Information Available: ^{1}H and ^{13}C NMR spectra of **2**−**7** and **9**−**22**, experimental details for ELLA inhibition tests, Figures S1−S5 from molecular dynamics simulations, force field parameters for triazole and hemiacetal derivatives, and FFTPDB reported with force field atom types, atom names, and RESP atomic charge values for each molecular fragment. This material is available free of charge via the Internet at http://pubs.acs.org.

JO071248A